1 OF 1
AD A
10606.

END
DATE
FILMED
11-81
DTIC

NPS67-81-010-

LEVEL

AD A106061

NAVAL POSTGRADUATE SCHOOL
Monterey, California

S DTIC
ELE
OCT 2 3 1981

A

COMBUSTION BEHAVIOR OF SOLID FUEL RAMJETS. Volume 1.
CORRELATION OF REACTING AND
NON-REACTING FLOW CHARACTERISTICS.

Brian A. /Binn, Winston E. /Scott, David W. /Netzer

Jul 81

Approved for public release; distribution unlimited.

Prepared for:

Naval Weapons Center
China Lake, CA   93555

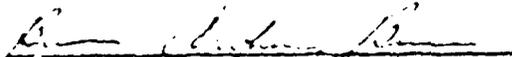81 10 23

NAVAL POSTGRADUATE SCHOOL
Monterey, California

Rear Admiral J. J. Ekelund   D. A. Schrady
Superintendent   Acting Provost

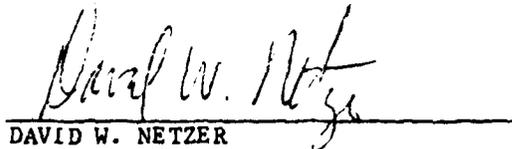Reproduction of all or part of this report is authorized.

This report was prepared by:

BRIAN A. BINN
Captain, U.S. Air Force

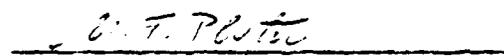WINSTON E. SCOTT
Lieutenant, U.S. Navy

DAVID W. NETZER
Professor of Aeronautics

Reviewed by: Released by:

M. F. PLATZER   W. M. TOLLES
Chairman of Aeronautics   Dean of Research

SECURITY CLASSIFICATION OF THIS PAGE (When Data Entered)

REPORT DOCUMENTATION PAGE		READ INSTRUCTIONS BEFORE COMPLETING FORM
1. REPORT NUMBER NPS67-81-010	2. GOVT ACCESSION NO. AD-A106 061	3. RECIPIENT'S CATALOG NUMBER
4. TITLE (and Subtitle) COMBUSTION BEHAVIOR OF SOLID FUEL RAMJETS VOL I. CORRELATION OF REACTING AND NON-REACTING FLOW CHARACTERISTICS		5. TYPE OF REPORT & PERIOD COVERED Final
		6. PERFORMING ORG. REPORT NUMBER
7. AUTHOR(s) Brian A. Binn, Winston E. Scott, David W. Netzer		8. CONTRACT OR GRANT NUMBER(s)
9. PERFORMING ORGANIZATION NAME AND ADDRESS NAVAL POSTGRADUATE SCHOOL MONTEREY, CA 93940		10. PROGRAM ELEMENT, PROJECT, TASK AREA & WORK UNIT NUMBERS N605308WR30053
11. CONTROLLING OFFICE NAME AND ADDRESS NAVAL WEAPONS CENTER CHINA LAKE, CA 93555		12. REPORT DATE July 1981
		13. NUMBER OF PAGES 58
14. MONITORING AGENCY NAME & ADDRESS(if different from Controlling Office)		15. SECURITY CLASS. (of this report) Unclassified
		15a. DECLASSIFICATION DOWNGRADING SCHEDULE

16. DISTRIBUTION STATEMENT (of this Report)

Approved for public release, distribution unlimited.

17. DISTRIBUTION STATEMENT (of the abstract entered in Block 20, if different from Report)

18. SUPPLEMENTARY NOTES

19. KEY WORDS (Continue on reverse side if necessary and identify by block number)

Solid Fuel Ramjet
Flow Characteristics

20. ABSTRACT (Continue on reverse side if necessary and identify by block number)
An experimental investigation was conducted to determine the relationship between the cold flow characteristics of velocity, pressure distribution, and turbulence intensity and the reacting flow performance and combustion characteristics of a solid fuel ramjet. The effects of configuration and air flow changes on the above characteristics were examined. Average regression rates and combustion efficiencies were not significantly affected by changes in configuration. These variations

DD FORM 1473   EDITION OF 1 NOV 65 IS OBSOLETE
1 JAN 73
S/N 0102-014-6601

in test conditions significantly affected the centerline turbulence intensity but not the near-wall turbulence intensity in cold flow. Near-wall turbulence profiles in cold flow were found to correlate with the fuel regression profiles in reacting flows. The use of bypass resulted in decreases in regression rate and efficiencies for all cases.

Accession For	
NTIS GRA&I	[X]
DTIC TAB	[ ]
Unannounced	[ ]
Justification	
By	
Distribution/	
Availability Codes	
Dist	Avail and/or Special
A	

TABLE OF CONTENTS

LIST OF FIGURES

LIST OF TABLES

SYMBOLS

A^* nozzle throat area

d_i initial diameter of fuel port

g_c gravity constant

M Mach number

$\dot{m}$ mass flow rate

P pressure

P_T stagnation pressure

R gas constant

$\dot{r}$ fuel regression rate

t_b burn time

T_t stagnation temperature

γ ratio of specific heats

Δw weight change of fuel grain

$\eta_{\Delta T}$ temperature rise combustion efficiency

ρ density

Superscripts

$-$ average value

Subscripts

4   nozzle entrance

p   primary air

s   secondary (bypass) air

T   total air

I. INTRODUCTION

The Naval Postgraduate School has had a continuing research effort directed at the combustion behavior of solid fuel ramjets under the sponsorship of the Naval Weapons Center, China Lake. Both mathematical modeling [Refs. 1, 2 & 3] and experimental efforts [Refs. 4-9] have been conducted to determine the effects of design variables on the obtainable performance. One major area requiring additional attention is the attainment of improved combustion efficiency together with higher energy fuels.

New fuels are required which will yield high density impulse and good flammability limits for various inlet, grain and aft mixing chamber configurations. Recently a wide variety of HTPB based fuels have been considered [Ref. 10 & 11]. To date the alternate fuels have not yielded significant performance improvements and indications are that mixing processes within the fuel grain port may be as important as fuel composition. The attainment of higher efficiencies with existing or new fuels may require innovative methods for controlled mixing of the diffusion limited combustion processes within the fuel port. However, there is some evidence from past work at NPS that variations in the curing process of Plexiglas has resulted in significant changes in combustion efficiency without additional mixing being attempted. Additional work is required to better understand the effects of fuel properties and mixing processes on the combustion efficiency.

It is important to determine fuel behavior under various operating conditions before final selection is made. In the past, fuels have been evaluated under limited test conditions. This has sometimes resulted in inexplainably low performance and unusual fuel regression patterns and/or

1

flammability limits in final hardware configurations.

Cold flow tests at UTC/CSD and NPS have been used for model validation efforts and to better understand the flowfield within the fuel grain and aft mixing chamber. However, these data have not been consistently related to fuel performance (regression pattern, efficiency, flammability limits, etc.) in a reacting environment.

It would be most beneficial if cold flow measurements and fuel characteristics could be used a priori to predict the expected fuel behavior in a reacting environment and in a specific geometric configuration.

In this investigation the performance of several fuels was measured under various operating conditions and test geometries and an attempt was made to correlate the results with cold flow measurements, fundamental fuel characteristics, and/or the amount of mixing induced near the fuel surface.

Volume I of this report presents the results obtained when an attempt was made to correlate cold flow measurements with reacting flow characteristics.

II. METHOD OF INVESTIGATION

In order to determine if relationships exist between cold flow
data and combustion performance, non-reacting flow data consisting of
static and total pressure measurements, and centerline and near-wall
hot-wire anemometer measurements have been made. Nominal test condi-
tions are listed in Table I. Static pressure was obtained with the
use of wall mounted taps along the length of the ramjet motor. These
values, along with stagnation pressure measurements from a total pressure
rake, were used to determine pressure distribution and velocity profiles
in the ramjet motor. The hot wire anemometer data yielded quantitative
and qualitative information on the turbulence intensity within the ramjet
model.

To gather the desired information from the reacting flow studies,
the solid fuel ramjet motor was mounted on a thrust stand. Along with
the thrust data, static pressure distributions along the grain were
obtained. The experimental firings were conducted using polymethylmeth-
acrylate (PMM) fuel grains. Nominal test conditions are presented in
Table I. Several grain modifications were also made to promote fuel-
air mixing within the fuel port.

3

TABLE I. NOMINAL TEST CONDITIONS

Figure: schematic diagram with labels D_r, D_i, h, D_o, $\dot{m}_s$, D_t, .0538, $\dot{m}_p$, $D_p = .0381$, L_r, .3048, .158, meters
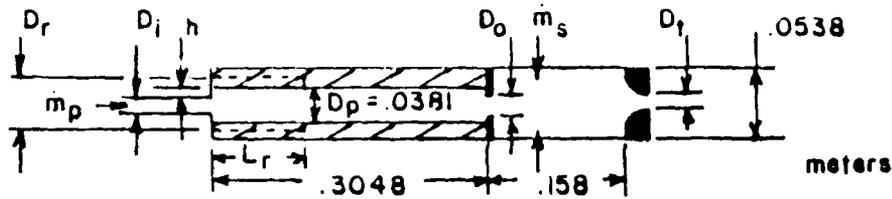
Config. No.	D_i(m)/D_o(m)	L_R(m)/D_R(m)	h/D_p	$\dot{m}_p$(kg/sec) / $\dot{m}_s$(kg/sec)	Cold Flow Data (D_t=.0127m)	Reacting Flow Exp (D_t=.0191m)
1	.0191/.0381	–	.250	.0907/0	x	
2+	.0191/.0381	–	.250	.0454/.0454	x	
3	.0127/.0381	–	.333	.0907/0	x	x
4	.0127/.0381	–	.333	.0454/0454	x	x
5++	.0191/.0381	–	.250	.0907/0	x	
6++	.0191/.0381	–	.250	.0454/.0454	x	
7++	.0127/.0381	–	.333	.0454/.0454	x	x
8	.0191/.0254	–	.250	.0907/0	x	
9	.0191/.0254	–	.250	.0454/.0454	x	
10	.0127/.0254	–	.333	.0907/0		x
11	.0127/.0254	–	.333	.0454/.0454		x
12	side dump	–	–	.0907/0	x	
13+++	.0127/.0381	–	.333	.0907/0	x	x
14*	.0127/.0381	–	.333	.0907/0		x
15	.0191/.0381	.1016/.0572	.250	.0907/0		x
16	.0191/.0381	.1524/.0572	.250	.0907/0		x

+ All bypass air runs: 2 dumps, 180° opposed, .0204 m dia., .0508 m. aft of fuel grain

++ Screen attached to inlet: 8x8 mesh (52 % open area)

+++ 11 circumferential grooves (.0254 m spacing) in fuel grain, .00635 m deep x .00635 m wide

* .0254 m dia. orifice midway in grain.

III. DESCRIPTION OF APPARATUS

A. RAMJET MOTOR

The solid fuel ramjet motor was that previously used by Mady, and others, at the U. S. Naval Postgraduate School[4-9]. The motor consisted of four main sections: the head-end assembly, the step insert section, the grain, and the aft mixing chamber/nozzle (Figure 1 and Table I).

The head-end assembly contained the inlets for the air, the ethylene inlet for ignition, and the nitrogen purge and the cooling air inlets. Two distinct types of head-end assemblies were used during the tests. For the initial cold flow measurements an axial air inlet was used upstream of the step inlet as shown in Figure 1. To conduct the hot firing experiments the ramjet motor was mounted on a thrust stand. This necessitated the use of a different head-end assembly to enable the air to enter the engine from the sides. The air was then turned 90° with a wedge to enter the inlet and fuel grain (Figure 2). Subsequent cold flow measurements were made using this inlet geometry.

The step insert section held the inlet in place. Two step inlets were used during this investigation, with inside diameters of 0.0127 and 0.0191 meters. These sizes resulted in h/D values of 0.333 and 0.25, respectively. The inlets were constructed such that a stainless steel 8x8 mesh (51.8% open area) screen could be attached at the grain inlet to vary the inlet distortion/turbulence intensity.

The cold flow tests and hot firings were done using the above mentioned PMM fuel grain. This fuel was selected because of its

availability and wide use for basic research in hybrid rocket combustion
and in studies of polymer degradation. The grains were nominally
0.3048 meters in length with an initial inside port diameter of 0.0381 m.

The aft mixing chamber had four bypass dumps located symmetrically
around the chamber. For this study two 180° opposed dumps were used,
and the remaining two were blocked off. These bypass dumps were
0.0204 m in diameter and were located 0.0508 m from the exit plane of
the fuel grain. A 0.0048 m thick orifice plate with a 0.0381 m internal
diameter was located at the aft end of the fuel grain to maintain
a fixed step height entering the aft chamber. A few tests were made
using an aft orifice with an internal diameter of 0.0254 m.

The aft chamber had a length to diameter ratio (L/D) of 2.93 and
an inlet step h/D of .146. A pressure tap was located near the rear
end of the aft chamber. A 0.0127 m diameter converging nozzle was used
in the cold flow experiments to provide choked flow. A nozzle of
0.0191 m diameter was used during hot firing runs to provide a chamber
pressure of approximately 4 atm.

B. AIR SUPPLY AND FLOW CONTROL SYSTEM

The main air supply was powered by a Pennsylvania air compressor
that could provide air at pressures up to 10 atm. The air was fed
into a reservoir and then directed to the ramjet motor. A Polytherm
air heater was also available if the air needed to be heated.

Standard ASME orifice flowmeters were used to measure the flow
rates of the air into the motor for both primary and secondary (bypass)
air. Manually operated gate valves between the orifices and the motor

6

were used to provide the desired flow rates to the motor. Two pneu-
matically operated Jamesbury ball valves (operating together) either
vented the primary air to the atmosphere, or allowed it to pass through
the motor. The line pressures and differential pressures across the
ASME orifices were recorded on a Honeywell Model 2106 Visicorder and/or
a strip chart recorder.

C. INSTRUMENTATION

Flow measurements during the cold flow tests consisted of a
total pressure rake, axial pressure distributions (using wall pressure
taps), and centerline and side wall hot wire turbulence intensity mea-
surements. During hot firings the axial pressure distribution was also
measured as was the thrust.

1. Total Pressure Rake

A 7-probe total pressure rake was designed to axially traverse
the ramjet motor from the inlet plane through the aft mixing chamber.
Figure 3 is a drawing of the rake installed in the PMM fuel grain.
A mounting device was attached to the nozzle to steady the probe and
allow for traversing of the motor. The probe support tube was scribed
for easy determination of probe location when inside the motor. Plastic
tubing connected the seven total pressure taps to a Scanivalve system,
which was in turn attached to a digital D.C. voltmeter for reading of
the data.

2. Static Pressure Taps

A total of 8 wall pressure taps were employed. One was located
in the head-end assembly and one, as previously mentioned, in the aft

mixing chamber. The remaining six were spaced in the fuel grains as shown in Figure 4. These were also connected to the Scanivalve system mentioned above. These measurements, along with the rake total pressure readings, allowed for determination of velocity profiles throughout the ramjet apparatus during non-reacting experiments. During non-reacting experiments the Scanivalve output was manually recorded. During hot firings the output was recorded on a strip chart with the Scanivalve cycled automatically.

3. Hot-Wire Anemometers

Turbulence intensity measurements were made during the cold flow experiments along the centerline of the ramjet motor and also along the side walls of the fuel grain at two circumferential positions (90° and 180°). The apparatus used miniature Thermo-systems Incorporated (TSI) hot wires. Figures 5 and 6 show the hot wire apparatus in the fuel grain. The hot wire was connected directly to the TSI electronic equipment. A D.C. voltmeter and a true RMS meter were used to read the hot wire output. Additionally, an oscilloscope was connected for visual observations of the hot wire output and for setting the stability prior to the measurements.

4. Thrust Measurement

Thrust measurement was accomplished by mounting the ramjet motor apparatus to a small thrust stand as shown in Figure 7. The head-end of the motor was mounted such that the thrust pick-up was in-line with the centerline of the engine. The transducer output was recorded on a strip chart recorder. Load cell calibration was accomplished using a pulley/weight system.

IV. EXPERIMENTAL PROCEDURES

A. CALIBRATIONS

The transducers required for the flow and thrust measuring devices were calibrated prior to the running of each test. The line pressure and differential pressure transducers and the Scanivalve were calibrated using a Heise gauge and bottled nitrogen.

B. NON-REACTING FLOW STUDIES

1. Pressure and Velocity Distributions

The total pressure rake was axially traversed from the air inlet plane to the aft mixing chamber. All 15 wall static and stagnation pressure readings, plus one atmospheric reading, were made when the rake was secured at each desired position. Data were taken at 0.0254, 0.0889, 0.1270, 0.2032, 0.3048, 0.3810 and 0.4445 m from the air inlet.

The wall static pressure distributions were obtained when the rake was positioned at 0.381 m (0.0762 m into the aft mixing chamber). This position was selected to limit effects due to the blockage which occurs when the probe is within the fuel grain.

The velocity profiles could easily be determined using the static and total pressure values together with the isentropic, compressible flow relationships between the pressures, velocity, temperature, and the properties of air. The values of γ and R, which were used, were those of air on a standard day at sea level.

2. Hot-Wire Anemometer Studies

A guide was mounted as close to the hot wire as possible to steady the probe. This helped reduce the vibration of the probe considerably. Although the readings taken near the rear end of the grain and in the aft mixing chamber did not receive the benefits from the guide, the velocities in these regions were much lower and vibrations of the probe were minimal.

The centerline turbulence intensity measurements were taken at the air inlet plane, at 0.0254 m intervals through the first half of the grain, and then at larger intervals (depending on the test being run).

The near-wall turbulence readings were taken at a nominal radial distance of 0.0024 m from the wall. Two passes were made down the grain in order to obtain the data at 90° and 180° under the same flow conditions. The data were recorded at 0.0127 m from the air inlet and then at 0.0254 m intervals to 0.2286 m with the experimental set-up used in these tests. If the probe guide had been allowed to exit the aft end of the grain, the wire would have broken when it came into contact with the wall.

Using the readings from the digital D.C. voltmeter and the Ballantine true RMS meter, the turbulence intensities were determined. Although the hot wire was used in the linearized mode, many of the measurements could only be considered in a qualitative manner since intensities often exceeded 15%.

C. REACTING FLOW STUDIES

The procedure for setting of the required flow rates for the tests was the same as that used in the non-reacting experiments.

10

The motor was ignited by first setting the desired air flow rate(s),
igniting a small ethylene-oxygen torch that vented in the face of the
step inlet, and then bleeding in a small amount of ethylene upstream
of the inlet dump. After ignition, the torch and ethylene bleed were
terminated.

Combustion normally lasted for forty-five seconds. The motor
was extinguished at the end of each run by simultaneously venting the
air to the atmosphere and actuating the nitrogen purge system. Low
pressure air was then blown through the motor for cooling.

1. Pressure Measurement

Several fuel grains were instrumented with pressure taps
identical to those in the non-reacting flow studies (Figure 4). As with
the cold flow tests, a fuel port pressure distribution was obtained.
The aft mixing chamber pressure (combustion pressure) was also recorded
on a Visicorder, in addition to the strip chart. This was necessary
to obtain a continuous pressure-time trace for the duration of the firing.
A highly accurate time signal was also recorded to allow determination
of burn time for regression rate calculations.

2. Temperature Measurement

The air inlet temperature was recorded on a strip chart. The
inlet total temperature was derived from the measured inlet static
temperature and the air flow rate. This was used, along with the derived
total temperature at the nozzle inlet, for computation of the combustion
efficiency.

3. Regression Rate/Pattern

To determine the average regression rate ($\bar{r}$) it was necessary to make preliminary measurements of the fuel grain prior to insertion into the ramjet motor. The grains were weighed prior to and after each run. Based on the weight loss and the burn time of the run the average regression rate was calculated using

$$\bar{r} = \frac{1}{2t_b} \left\{ \sqrt{\frac{4\Delta w}{\rho_f g_c \pi} + d_i^2} - d_i \right\} \qquad (1)$$

Average initial diameter values ($\bar{d}_i$) for the PMM fuel grains with piecewise varying internal geometries were computed. This computation was based on equating the total calculated internal volume V_t to that of an equivalent centrally perforated, constant diameter fuel grain.

The regression patterns, axial and circumferential, were also of interest during this study. The regression patterns were examined by making selective cuts through the fuel grain both perpendicular and parallel to the central axis. These profiles were inspected for location of maximum regression rate and symmetry of burn pattern.

4. Thrust Measurement

The ramjet motor was mounted on a small thrust stand to measure thrust directly. The thrust transducer was connected to a strip chart recorder. A small tare was used to assure solid contact of the thrust stand against the transducer at all times. The thrust measurement was also used with other measured variables to determine combustion efficiency.

5. Calculation of Combustion Efficiencies

The efficiency of the ramjet combustion process is usually defined as a ratio of the theoretical temperature rise to that which is actually attained. Because of the difficulty in measuring an average gas temperature due to the high temperature levels, the accepted practice is to calculate the temperature of the gas based on either burner pressure or thrust.

The measurement of thrust can be suspect depending on the experimental set-up and measuring technique. One of the main problems is the bringing of the air flow into the ramjet motor while mounted on the thrust stand. It is possible to introduce an unknown tare force which can degrade the acceptability of the measured thrust. The experimental set-up minimized this problem by bringing the air into the head-end and aft mixing chamber through long flexible hoses from above, thereby imparting no force along the thrust line of the motor.

To determine the temperature rise efficiency the following relationship was used:

$$n_{\Delta T} = \frac{T_{t\ meas} - T_{t\ air}}{T_{t\ theor} - T_{t\ air}} \qquad (2)$$

$T_{t\ air}$ was determined from measurement of the temperature at the head-end of the motor. In this low velocity region, stagnation and static temperatures are virtually identical. The value of $T_{t\ meas}$ can be found using the measured pressure and mass flow rate, as previously mentioned,

13

and the one-dimensional mass continuity relationship for flow through a choked nozzle. From

$$\dot{m}_T = \frac{P_{T4} \, A^*}{\sqrt{R \, T_{T4}}} \sqrt{\gamma g_c \left(\frac{2}{\gamma + 1}\right)^{(\gamma+1)/(\gamma-1)}} \qquad (3)$$

the following relationship can be obtained:

$$T_{t \; meas} = \left(\frac{g_c \, \gamma}{R}\right)\left[\left(\frac{2}{\gamma + 1}\right)^{\frac{\gamma+1}{\gamma-1}}\right]\left[1 + \left(\frac{\gamma - 1}{2}\right)M_4^2\right]^{\frac{2\gamma}{\gamma-1}}\left[\frac{P_4 \, A^*}{\dot{m}_T}\right]^2 \qquad (4)$$

Values of P_4, A^*, AND $\dot{m}_T$ are measured quantities (station 4 is just prior to the nozzle). The NWC Pepcode computer program was used to determine the theoretical combustion temperature and required gas properties $(R$ and $\gamma)$ at the experimentally determined air-fuel ratio and inlet conditions. M_4 was determined from γ and the known nozzle contraction ratio.

14

V. RESULTS AND DISCUSSION

A. NON-REACTING FLOW EXPERIMENTS

The non-reacting flow experiments were accomplished in an attempt
to characterize the flowfield within the solid fuel ramjet motor for
widely varying geometries and flow rates. The studies included the
determination of velocity profiles, wall static pressure variation,
centerline turbulence intensity, and near-wall turbulence intensity.
The magnitude of the RMS voltage/DC voltage measured with the hot-wire
anemometer (in the linear mode) was normally greater than 15% and,
therefore, cannot actually be called "turbulence intensity". The ratio
only provided relative magnitudes from test to test. For discussion
purposes, however, the term "turbulence intensity" will be employed

1. Large Inlet Diameter (Configurations 1 and 2, Table I)

The reattachment point/region can be considered to be that point
where no reverse flow occurs. This occurred at approximately 0.102 m
for the case with no bypass as compared to over 0.203 m when bypass was
introduced (Fig. 8 and 9). The reattachment point location for no
bypass flow compared favorably with previous work (Fig. 10). The
length of the recirculation region for the run with bypass was sur-
prisingly long. If the flow were laminar there would be a tendency for
the reattachment zone to move downstream. However, a check of the
Reynolds number indicated that, as expected, the flow was fully turbulent.
Apparently, when small recirculation regions are employed the flow
characteristics within the aft mixing chamber affect the recirculation

15

region within the fuel port. The velocity profiles in the center portion of the aft mixing chamber were flat and essentially identical for both cases.

Figure 11 presents the axial pressure distributions in the fuel grain and one point in the aft mixing chamber. The pressure leveled off at about 0.127 m without bypass, slightly downstream of reattachment. The bypass pressure distribution was quite flat over the entire grain length but did decrease slightly at the head-end.

Peak turbulence "intensities" along the motor axis were located at approximately 0.140 m and 0.191 m for the no-bypass and bypass configurations respectively, just downstream of the locations where wall static pressures leveled off and reattachments occurred (Fig. 12). Bypass caused higher values of turbulence "intensity" in the aft region of the fuel grain.

Analysis of the side and bottom wall turbulence "intensities" (Fig. 13 and 14) indicated that, in contrast to the centerline turbulence "intensities", there was no significant effect of the bypass on the position of maximum near-wall turbulence "intensity" in the fuel port. Bypass levels were again greater than no-bypass levels. Secondary peaks of turbulence "intensity" occurred at approximately 0.102 m, near where the flow reattachment occurred with no bypass. The near-wall turbulence "intensities" were significantly greater than the centerline values. Comparison of side and bottom wall profiles indicated that the flow was nearly symmetric along the grain.

The upstream effects of the bypass on the flow seems to be significant. It moved the reattachment point downstream (as determined by the

16

mean velocity profiles), increased the required distance for the velocity
profiles to become flat, moved the peak centerline turbulence "intensity"
downstream, and also caused an increase in the turbulence "intensities"
for both near-wall and centerline positions.

If centerline turbulence "intensity" affects the regression rate
pattern, the results indicate that a more rapid variation in regression
rate would occur along the grain for 50% bypass. It could also be
expected that the point of maximum fuel regression would take place
farther downstream for the bypass case. However, if near-wall turbu-
lence is dominant in its effects on the regression pattern no signifi-
cant variation would be expected between no bypass and 50% bypass.

2. Large Inlet Diameter, w/Screen, (Configurations 5 and 6, Table I)

This test was conducted with a wire mesh screen attached to
the step inlet in order to examine the effects of inlet distortion/
turbulence intensity variations. Velocity profiles (Fig. 15) and
a pressure distribution (Fig. 16) are presented for the no-bypass
conditions.

The velocity profiles were almost identical to those with no screen;
showing only a slight decrease in maximum velocity at the inlet. The
screen did not seem to have any effect on the reattachment point location
or the mean velocity profiles.

The pressure distribution (Fig. 16) also exhibited the same
characteristics as the inlet without the screen.

The effect of the screen was readily noticeable in the turbulence
"intensity" measurements (Figs. 17-19). The location of the peak
centerline "intensity" was the same, but the value was much greater.

17

Since the average velocity (U) was nearly the same with or without the screen, the fluctuating velocity values (u') were much greater As for the inlet without the screen, the peak near-wall "intensities" occurred farther upstream than the peak centerline "intensities." The screen had little effect on the magnitude of the bottom wall "intensities" but decreased the side wall values.

The screen apparently introduced increased centerline turbulence without significantly affecting the mean flow characteristics or the near-wall turbulence.

3. Large Inlet Diameter, w/aft Orifice Plate (Configurations 8 and 9, Table I)

In this series of experiments a small diameter orifice plate was placed at the rear of the grain. This geometry should provide increased mixing of the fuel vapor and air within the aft end of the fuel port.

The wall static pressure data used to construct the velocity profiles showed large fluctuations, and a drop in mean pressure at the aft end of the grain where the flow accelerated through the small orifice. The mean velocity profiles within the fuel grain were the same as without the plate (Fig. 16 and 20). The aft-end flow restriction apparently caused large scale oscillations in the flow within the entire fuel grain. The mean location of the reattachment point appeared to be unchanged. A difference was noted in the aft mixing chamber, as expected, since the inlet flow area was reduced by the presence of the plate. Near the grain exit and into the aft mixing chamber, the velocity increased and a large aft recirculation zone was generated.

18

The centerline turbulence (Fig. 21) was also affected by the installation of the plate. The turbulence "intensity" without bypass did not peak and then drop off as it did without the plate. The values increased to a slightly higher value and remained nearly constant. The bypass condition showed a great increase in turbulence "intensity" within the fuel grain, indicating again that the fluctuating velocity (u') was much greater.

The near-wall turbulence "intensity" profiles (Figs. 22 and 23) were nearly the same with and without the orifice plate, with peak "intensity" occurring at about 0.102 m. It is interesting to note that the wall measurements showed the turbulence "intensity" to drop off after the peak value whereas the centerline values did not. The near-wall "intensity" values were very similar in magnitude and profile with and without the aft orifice plate. These data indicate that the effect of the plate on the higher frequency turbulence might be confined to the core of the flow and to the aft mixing chamber. As noted above, very low frequency mean velocity oscillations were introduced in the flow by the aft orifice plate. Thus, increased bulk mixing occurred throughout the fuel port and increased centerline turbulence occurred in the flow at the aft end of the fuel grain where the boundary layer is thick. This behavior could indicate that the orifice plate may increase fuel regression rate near the aft end and also may increase combustion efficiency. However, if near-wall turbulence dominates the regression rate behavior, very little regression rate changes would be observed.

19

4. Small Inlet Diameter (Configurations 3 and 4, Table I)

Figures 24 and 25 depict the velocity profiles obtained with and without bypass, respectively. Both conditions of air flow exhibited similar profiles with flow reattachment occurring between 0.089 and 0.127 m. Reattachment location has been shown previously to be a function of step height[5]. It was not possible from this data to locate a more precise position. Later measurements in the motor, with the thrust stand mounted air inlet configuration, indicated a reattachment point at 0.122 m without bypass and 0.109 m with bypass. Bypass did not cause the large scale recirculation effects on the velocity profiles within the fuel grain as it did with the large diameter inlet. The "profiles" in the aft mixing chamber apparently represent large scale recirculation in this region, with or without bypass. This is a marked deviation from the results of the experiments using the larger inlet.

The axial pressure distributions (Fig. 26) show the same general characteristics as obtained with the large inlet. These results indicate that bypass has more upstream effects on the large diameter/lower velocity inlet, but that the aft mixing region is more unsteady with the small diameter inlet.

Centerline and near-wall turbulence "intensities" are shown in Figures 27 through 29. The general characteristics of the centerline "intensity" profiles were in agreement with that from the large inlet. The magnitudes of the centerline "intensities" were considerably greater, as might be expected from the higher shear forces in the forward region. Without bypass, the peak centerline "intensity" occurred further upstream, very near flow reattachment. The introduction of the

20

bypass air flow increased the values of the "intensity", especially in the aft portion of the grain, and the values were much higher than with the large inlet. The highest value of centerline turbulence "intensity" with bypass occurred downstream of the flow reattachment and the location where the pressure leveled off.

Near-wall turbulence "intensities" were smaller with the smaller inlet and the peak values occurred further downstream. Bypass did not affect the location of the peak near-wall turbulence.

Higher centerline values and lower wall values, as compared to the larger inlet diameter, can be explained by the movement and location of the eddies created by the interface between the core flow and the recirculation region. The eddies formed are closer to the centerline with the small inlet and are of greater intensity initially. This could explain the occurrence of the peak centerline "intensity" closer to the head-end, and the greater value without bypass air. Apparently, the larger initial eddies are dissipated rapidly as they approach the wall, since near-wall turbulence "intensity" was lower with the smaller inlet.

The effects of these data on the expected fuel regression rates and regression pattern depends upon whether centerline or near-wall turbulence "intensity" (or both) is more significant. If regression rate is a stronger function of centerline turbulence "intensity" the position of highest regression could be expected to occur at the aft end of the grain when bypass air is introduced. If near-wall "intensity" is predominant, the maximum regression rate would occur at about midgrain. The downstream shift of peak near-wall turbulence "intensity"

21

with increasing h/D is in agreement with reattachment and regression rate behavior.

The turbulence data shown in Figures 27, 28 and 29 were obtained with an axially directed and straightened flow entering the fuel inlet dump (Fig. 1). Also shown on Figures 27 and 28 are turbulence profiles obtained with rapidly turned, 90° opposed dumps upstream of the fuel inlet dump (Fig. 2). The latter geometry is seen to significantly increase both centerline and near-wall turbulence levels. The peak in the center-line turbulence profile was shifted downstream. However, the near-wall turbulence profile was not affected.

    5. <u>Small Inlet Diameter, w/Screen (Configuration 7, Table I)</u>

The results obtained with the screen on the small diameter inlet with bypass were somewhat different from those obtained when the screen was attached to the large diameter inlet. Centerline turbulence increased to very large values and peaked near the aft end of the fuel grain (Fig. 30) as it did without the screen (Fig. 27). The location of the maximum near-wall turbulence "intensity" moved upstream to approximately 0.10 m. The location of the flow reattachment (approximately 0.109 m) was not significantly affected by the screen.

    6. <u>Circumferentially Grooved Fuel Grain (Configuration 13, Table I)</u>

Since earlier data have indicated that alternate fuels may not provide improved performance in conventional centrally perforated fuel grains, a fuel grain modification to enhance near-wall mixing was investigated. Circumferential grooves were cut into the PMM fuel grain in order to disturb the boundary layer and to somewhat increase the fuel-air mixing in the reaction region (Table I).

22

The mean velocity profiles and reattachment points were not significantly different from those obtained without the grooves. Figures 30 and 31 present the non-reacting flow turbulence profiles for identical grain inlet flow conditions with and without the enhanced near-wall mixing. The grooves increased near-wall turbulence over much of the forward part of the fuel grain and increased the centerline turbulence in the aft portion of the fuel grain.

B. REACTING FLOW EXPERIMENTS

A total of 28 firings were conducted, all with PMM fuel grains having a nominal length of 0.305 m (12 in.). Nominal ignition and run times were 3 seconds and 45 seconds respectively.

Calculated values of regression rate and temperature rise efficiency based on pressure are presented in Table II. Since all tests were conducted using a fixed fuel grain length and total air flow rate, the equivalence ratios for the bypass tests were considerably less than for nonbypass tests.

23

TABLE II

DATA FROM REACTING FLOW EXPERIMENTS

Description	Non-bypass							Bypass				Bypass + Inlet Screen				Non-bypass + small aft orifice				Bypass + small aft orifice			Non-bypass grooved grain		Non-bypass aft-grain orifice		Non-bypass enlarged grain inlet	
Test No.	1	2	3	4	5	6	7	8	9	10	11	12	13	14	15	16	17	18	19	20	21	22	23	24	25	26	27	28
Config. (TABLE 1)	3							4				7				10				11			13		14		15	16
$\dot{m}_p$ (kg/sec)	.093	.089	.088	.086	.089	.089	.087	.051	.051	.051	.037	.049	.050	.033	.055	.091	.090	.088	.066	.049	.051	.037	.084	.089	.082	.090	.089	.095
$\dot{m}_o$ (kg/sec)	0	0	0	0	0	0	0	.048	.049	.050	.033	.048	.049	.027	.058	0	0	0	0	.048	.049	.030	0	0	0	0	0	0
$\bar{r}_{fuel}$ (m/sec$\times 10^5$)	1.62	1.67	1.67	1.85	1.60	1.50	1.57	1.17	1.25	1.17	0.86	1.18	1.12	0.91	1.22	1.67	1.75	1.66	1.63	1.38	1.25	0.97	1.91	1.97	1.65	1.67	1.22	
$(\dot{m}_p+\dot{m}_o)/\dot{m}_{fuel}$								17.58	16.56	16.95	16.95	17.6	18.2	13.89	19.08					14.4	15.6	14.71						
$\dot{m}_p/\dot{m}_{fuel}$	11.34	10.83	10.31	8.93	11.11	11.36	11.20	9.01	8.29	8.62	9.01	8.92	9.26	7.58	9.31	10.79	10.25	10.16	10.53	7.32	8.00	8.13	7.75	8.20	9.52	10.8	12.5	14.3
P_c (atm)	3.66	3.59	3.68	3.64	3.66	3.69	3.73	3.18	3.31	3.26	2.31	3.21	3.23	2.28	3.69	3.68	3.76	3.47	3.52	3.40	3.41	2.29	3.99	4.17	3.54	3.58	3.57	3.22
$\eta_{\Delta T_{prass}}$	85.4	84.9	89.9	79.7	90.1	92.2	84.8	77.6	79.2	76.6	79.7	82.7	82.3	92.0	86.2	85.2	88.4	76.8	86.5	79.7	81.3	77.5	86.4	90.0	88.4	79.3	94.2	65.1

1. Small Inlet Diameter (Configurations 3 and 4, Table I)

     As expected with this type of axial inlet, the regression

pattern was circumferentially symmetric at all points along the grain.

This was true for all firings accomplished. The non-bypass point of

maximum regression (Fig. 32) was located at approximately 0.13 m from

the head-end. From the cold flow data for the same geometry (Figs. 27,

28-solid symbols), this peak occurred near the peak in near-wall turbu-

lence "intensity".

     The firings with 50% bypass produced efficiencies approximately

8 points lower than the non-bypass results (fixed grain length and total

air flow rate). However, the point of maximum regression rate was un-

changed (Fig. 32); also in agreement with the near-wall turbulence behav-

ior. The regression rate did not decrease as rapidly from the maximum

point to the aft end compared to that for the non-bypass conditions.

The cold flow centerline turbulence (Fig. 27) continued to rapidly

climb in the aft portion of the grain. If centerline turbulence affects

the wall regression rate, the latter would be expected to continue to

increase with axial distance. Bypass did cause the near-wall turbulence

to level-off toward the aft end of the fuel grain (Fig. 28). Near-wall turbulence intensities were also slightly higher for the case with bypass. These results indicate that near-wall turbulence "intensity" better correlated with regression behavior than did centerline turbulence "intensity". This could be expected since the fuel layer is quite thin and the flame is normally located very near the wall. Turbulence/mixing within the hot gas core apparently has little effect on the fuel regression rate.

2. <u>Small Inlet Diameter, w/Screen, (Configuration 7, Table I)</u>

The test with no bypass air flow would not sustain combustion. Combustion was attained for the case of 50% bypass. For cold flow, the screen was observed to significantly increase the centerline turbulence intensity. This amount of turbulence apparently greatly affected the mass transport of air into the recirculation region. This could possibly cause the normally fuel rich recirculation zone to be saturated with air, thereby quenching the combustion reaction. The reduction of the air inlet velocity (mean and fluctuating component) with the use of bypass was apparently enough to allow the flameholder to sustain combustion in the grain.

Use of the inlet screen resulted in a slight increase in efficiency for those tests with nominal flowrates. Two tests (14 & 15) with low or high air flow rates did produce significantly higher efficiencies. The inlet screen had no noticeable effect on the average regression rate of the fuel grain (Table II). However, there was a large difference in the location of the point of maximum regression. This was located at approximately 0.07 m (vs. approximately 0.13 m with no screen)

26

from the head-end and was more sharply defined than the case without the screen (Fig. 32).

The upstream movement of the position of maximum regression rate and the decreased regression rate near the aft end of the grain was again in good agreement with the behavior of the near-wall turbulence distribution (Fig. 31).

3. Small Inlet Diameter, w/Aft Orifice Plate, (Configurations 10 and 11, Table I)

The inclusion of the smaller diameter aft orifice plate did not appreciably change the performance of the ramjet motor in either the non-bypass or bypass flow conditions as compared to the motor with the larger diameter orifice plate. One test (No. 18) had very low efficiency.

4. Circumferentially Slotted Fuel Grain (Configuration 13, Table I)

Only two tests were conducted with this configuration. The increased fuel-air mixing near the fuel surface significantly increased the fuel regression rate (Table II) but did not affect the combustion efficieny. Too much mixing can quench chemical reactions and decrease combustion efficiency and too little mixing can reduce combustion efficiency by allowing excessive unburned fuel vapor/carbon to enter the aft mixing chamber.

Regression rate profiles with and without the grooves are presented in Figure 32. The grooves did not affect the position of the maximum regression rate but did slightly increase the profile in the forward and aft portions of the grain. This behavior corresponded more nearly to the near-wall turbulence profile (Fig. 31) than to the centerline turbulence profile (Fig. 30). Apparently, the grooves provided increased fuel sur-face area but did not significantly affect the diffusion flame zone.

27

5. Centrally Located Orifice Plate in Fuel Grain (Configuration
    14, Table I)

In order to compare the effects of large scale mixing to those
obtained with near-wall mixing, a fuel grain was modified to include
an orifice plate midway in the grain. Although the resulting fuel
regression pattern was very non-uniform (high regression near orifice
plate), no significant change in average regression rate or combustion
efficiency was obtained (although test No. 26 did have lower efficiency).

6. Enlarged Forward End of Fuel Grain (Configurations 15 and 16,
    Table I)

Another means of increasing mixing and at the same time
decreasing grain inlet flow velocity is to enlarge the inlet dump
and initial fuel grain diameters (to maintain an adequate area ratio
for flame stabilization). Test 27 (Table II) utilized an enlarged
inlet diameter with a length approximately equal to the recirculation
zone length. Test 28 (Table II) used a significantly longer enlarged
inlet region. Both tests resulted in significantly reduced fuel
regression rates. Combustion efficiency was not significantly affected
in Test 28. The high value obtained in Test 27 may be misleading since
large amplitude combustion pressure oscillations were present.

7. Combustion Pressure Oscillations

The peak-to-peak amplitude of the pressure oscillations are
typically less than 3% for the non-bypass conditions. This was also
true for the grooved fuel grain. All tests with bypass had signifi-
cantly greater pressure oscillations. The frequency and/or amplitude
could not be determined precisely because of the recording speed and

the line length connecting the motor to the pressure transducers. In similar tests, Mady[6] reported the frequency to be about 150 Hz. and the amplitude to be approximately 20% of chamber pressure in the bypass configuration. The magnitude of the oscillations observed in the present tests were approximately 10% of the chamber pressure. This behavior appears to be linked to the interaction of the bypass air with one of the shear layers (exiting the fuel grain or at the air inlet). The smaller aft orifice plate also caused an additional characteristic. Combustion oscillations occurred periodically (approximately every 6 seconds) for short periods of time. This showed up as small peaks in the pressure and thrust-time traces.

When the forward end of the grain was enlarged for a length approximately that of the recirculation zone, small amplitude (3% of P_c) oscillations transitioned to larger (10% of P_c) amplitudes after 20 seconds of burn time. When the enlarged diameter was lengthened to be greater than the recirculation zone length, the pressure oscillations began at a low amplitude (5% P_c) and increased gradually (to 10% P_c) until shutdown (at 45 seconds burn time).

These data indicate that combustion pressure oscillations can occur in solid fuel ramjets as a result of induced disturbances to the fluctuating shear layers at the fuel grain and aft mixing chamber inlets. Further studies of this phenomena are currently being conducted.

29

VI. CONCLUSIONS

1. Geometric changes to the solid fuel ramjet which result only in increased core-flow turbulence do not significantly affect fuel regression rate or combustion efficiency.

2. Non-reacting flow measurements of near-wall turbulence "intensity" profiles appear to reasonably correlate with measured fuel regression profiles in the reacting environment.

3. Utilization of grooves in the fuel surface increased near-wall turbulence in the head-end of the fuel grain but did not affect combustion efficiency.

4. If enhanced/controlled mixing within the fuel port is to result in increased combustion efficiency it probably will have to be introduced very close to the diffusion flame zone.

5. Bypass air has more effect on the flow upstream (within the fuel port) as the inlet step height is decreased.

6. Combustion pressure oscillations appear to be the result of induced disturbances to the shear layers that are present at the entrance sections of the fuel grain and the aft mixing chamber.
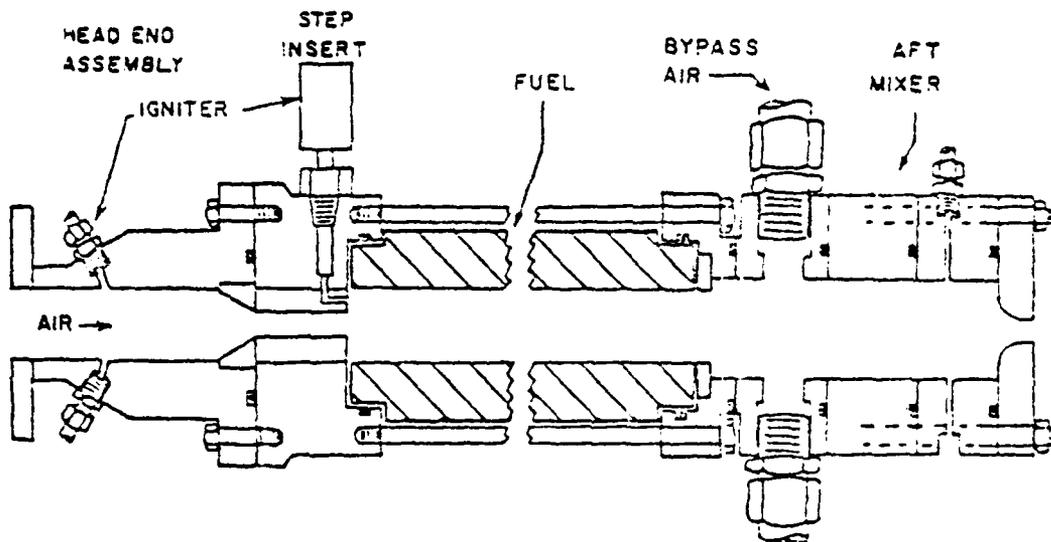
Fig. 1   Schematic of Solid Fuel Ramjet
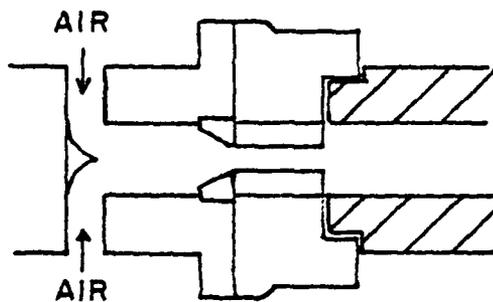
Fig. 2   Schematic of Air Inlet System for Engine on Thrust Stand

31
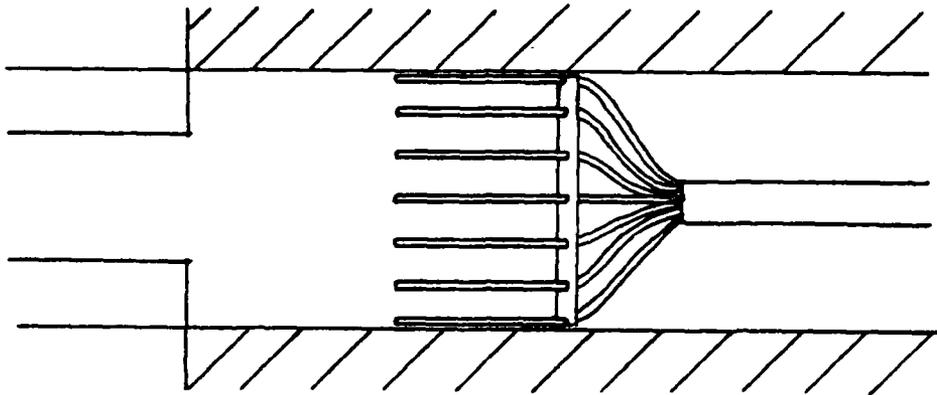
Fig. 3.   Total Pressure Probe in Fuel Grain
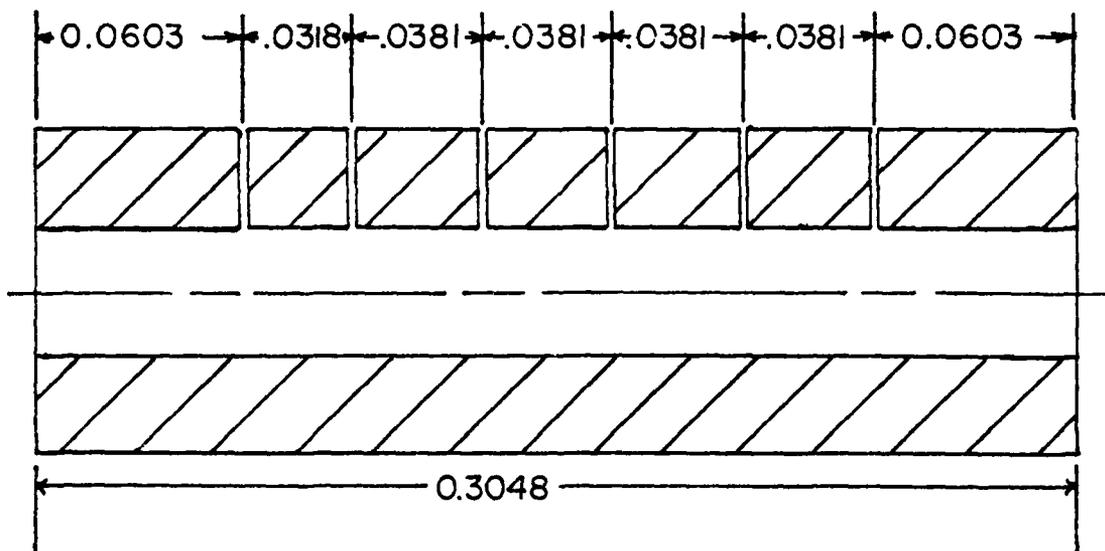
Fig. 4.   Pressure Tap Locations in PMM Fuel Grain
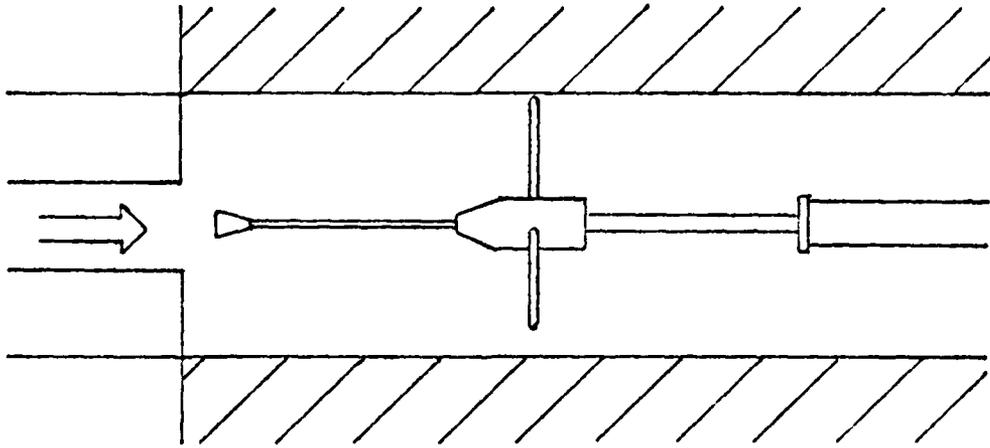
Fig. 5.   Centerline Hot Wire Probe
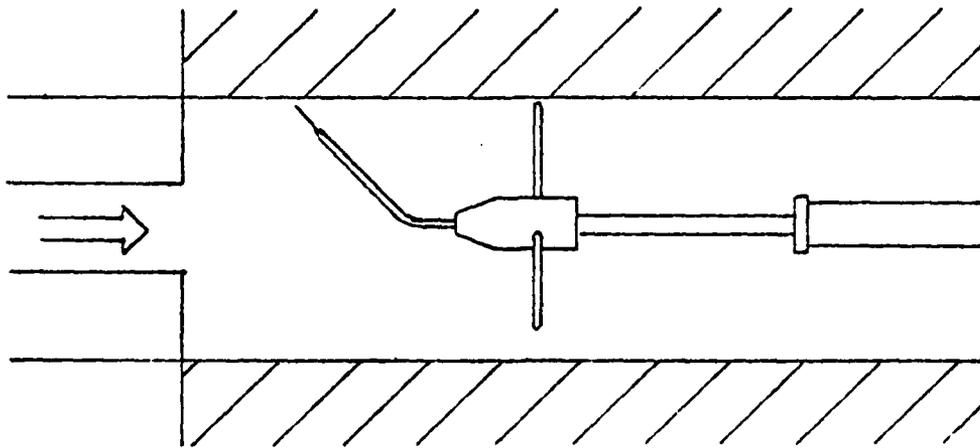
Fig. 6.   Near-Wall Hot Wire Probe

33
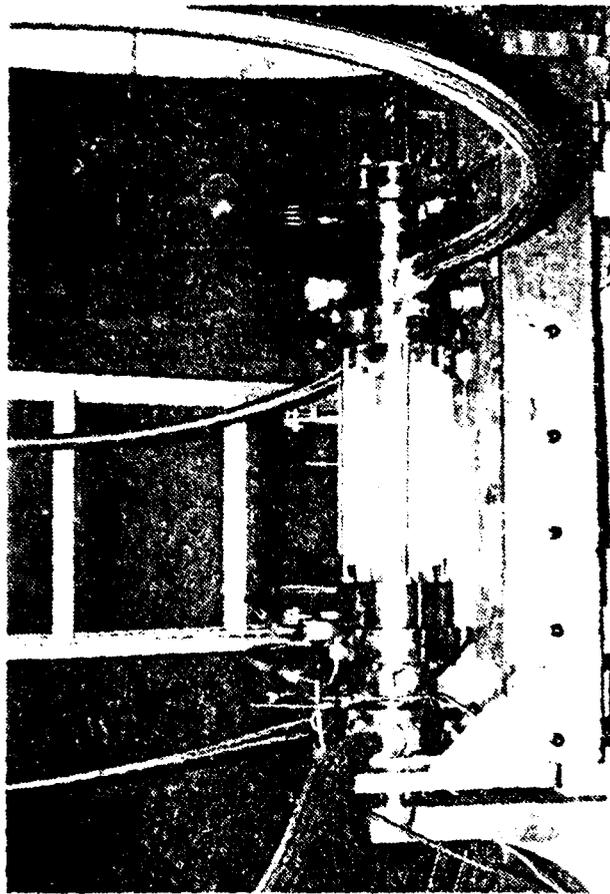
Figure 7. Solid Fuel Ramjet on Thrust Stand

34
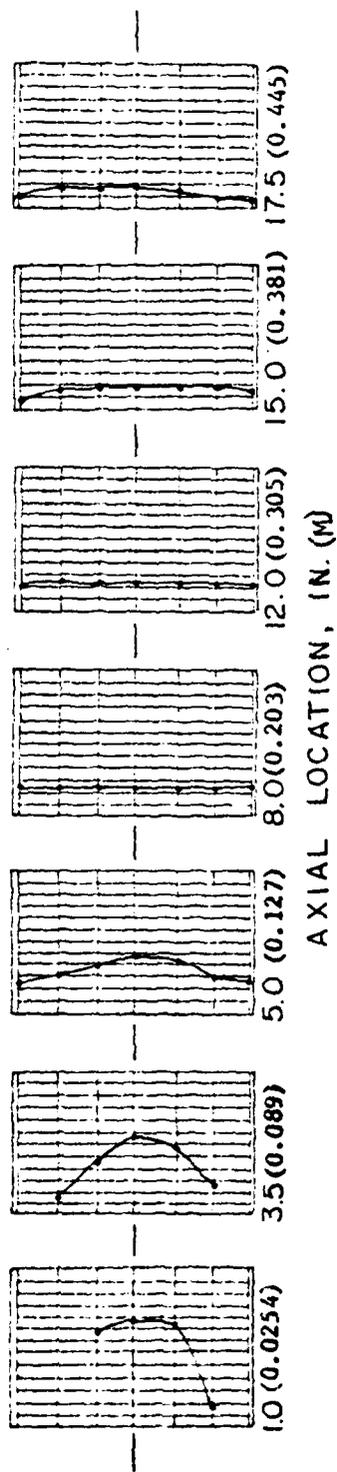
Fig. 8. Velocity Profiles, No-Bypass (Config. 1, Table I), P_c = 3.80 atm, $\dot{m}_p$ = 0.090 kg/sec

(1 Div. = 25 fps)

AXIAL LOCATION, IN. (M)
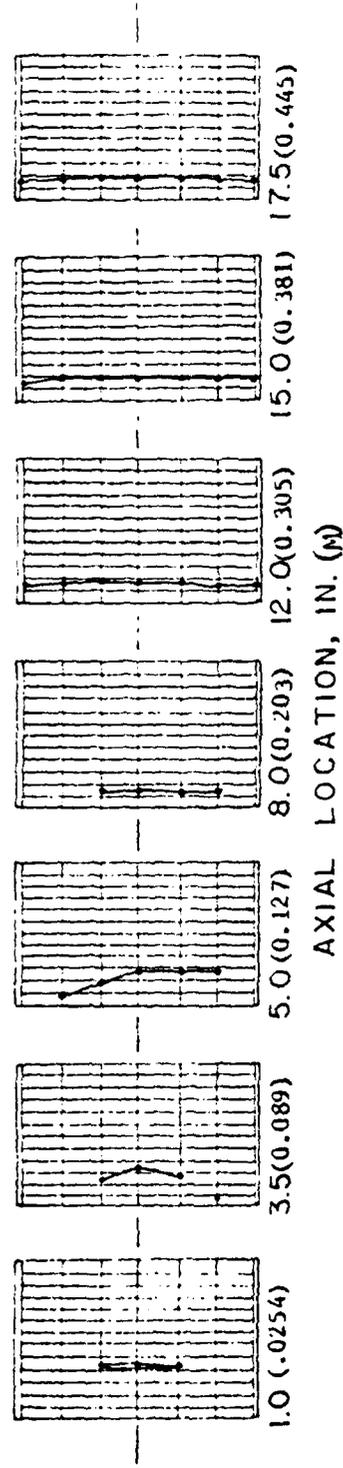
Fig. 9. Velocity Profiles, Bypass (Config. 2, Table I), P_c = 3.84 atm, $\dot{m}_p$ = 0.047 kg/sec, $\dot{m}_s$ = 0.046 kg/sec (1 Div. = 25 fps)

AXIAL LOCATION, IN. (M)

35

	KRALL-SPARROW Maximum heat transfer
	RAMJET MODEL
	PHANEUF-NETZER 10% Blowing
	PHANEUF-NETZER No Blowing
	BOAZ-NETZER Water injection
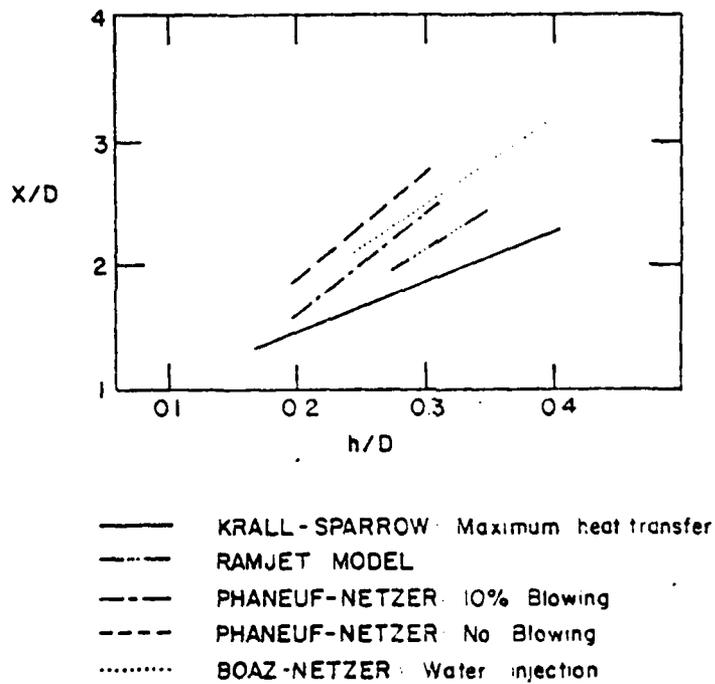
Fig. 10. Reattachment Locations for Axisymmetric Flows
(Fig. 7 from Ref. 7)
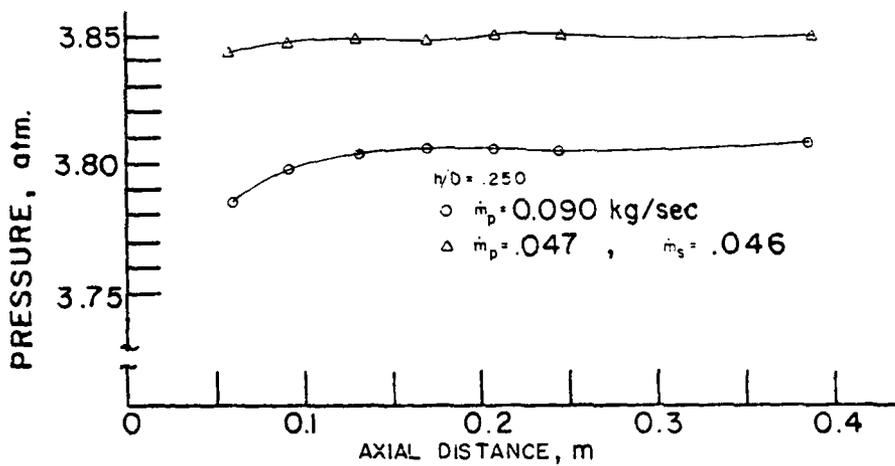
Fig. 11. Axial Pressure Distributions, h/D = 0.250

h/D = .250
O $\dot{m}_p$ = 0.092 kg/sec
△ $\dot{m}_p$ = 0.046 kg/sec, $\dot{m}_s$ = 0.045 kg/sec

FUEL GRAIN

AXIAL POSITION, m

TURBULENCE "INTENSITY"
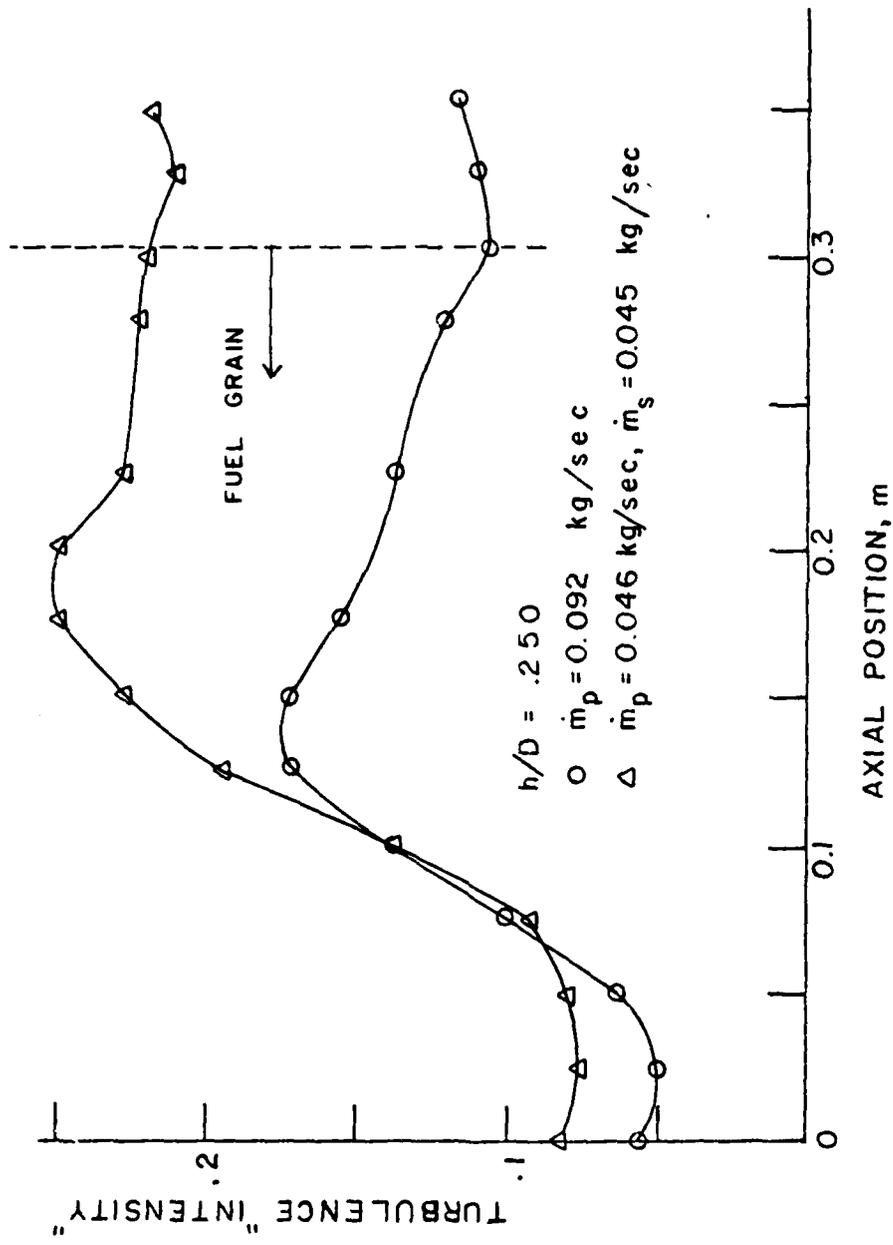
Fig. 12. Centerline Turbulence Intensity, h/D = 0.250

38
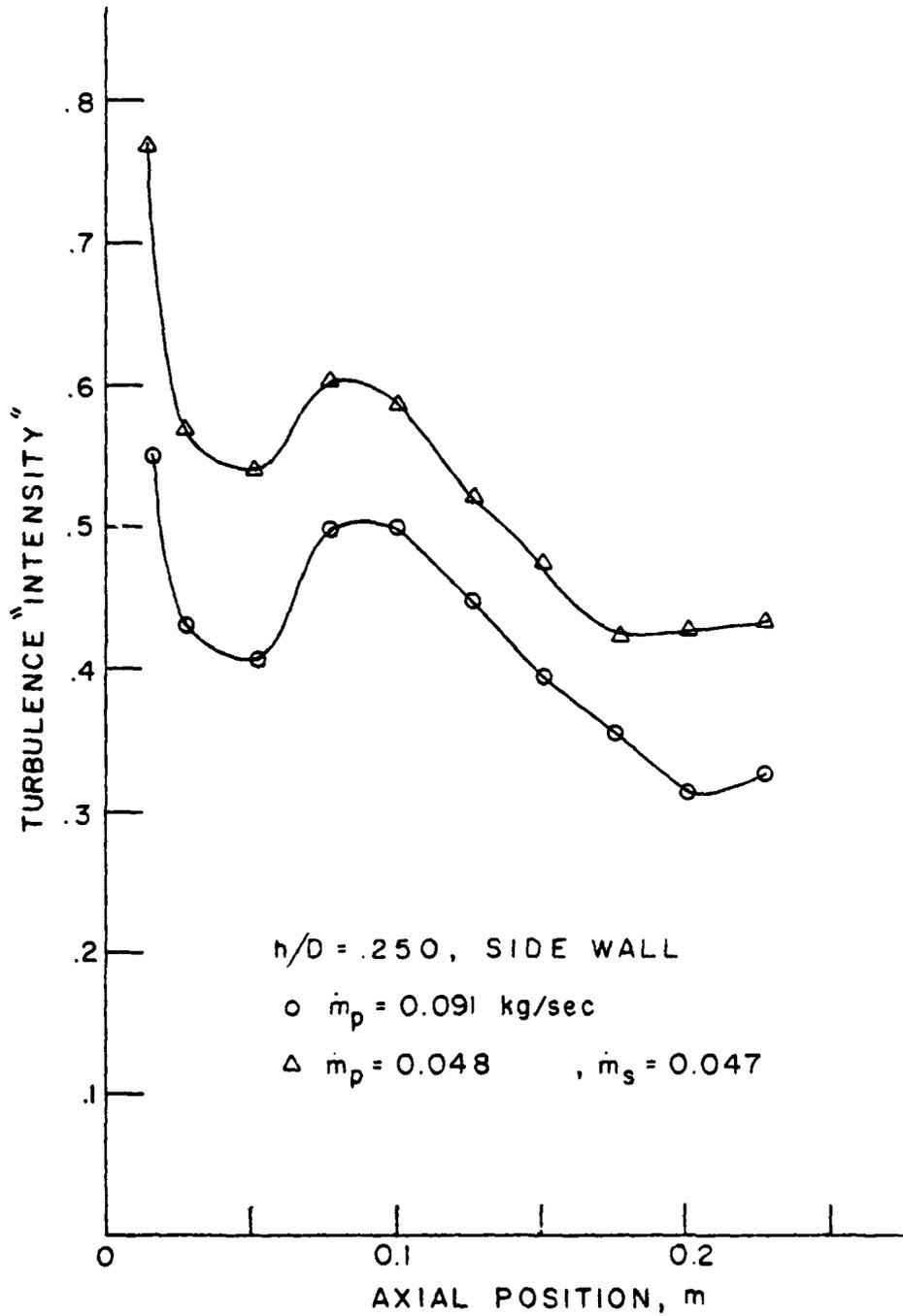
Fig. 13.   Side Wall Turbulence Intensity, h/D = 0.250
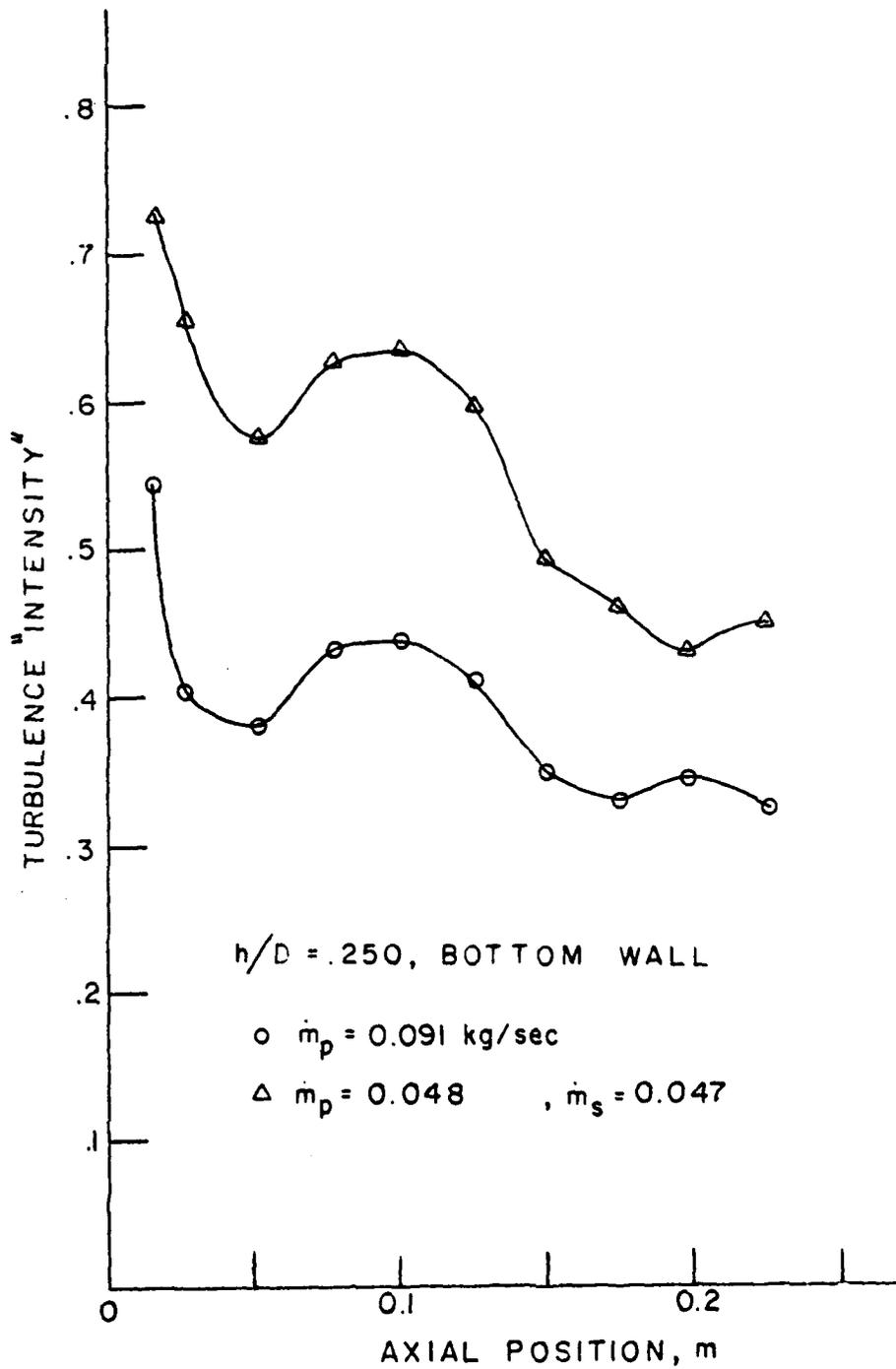
Fig. 14.   Bottom Wall Turbulence Intensity, h/D = 0.250
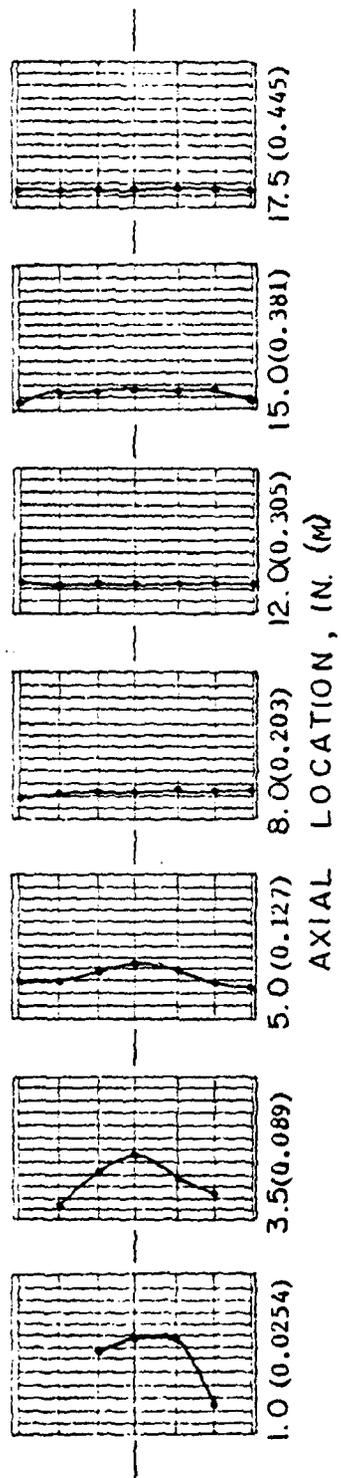
Fig. 15. Velocity Profiles, (Config. 5, Table I), w/Screen, P_c = 3.96 atm, $\dot{m}_p$ = 0.093 kg/sec

(1 Div. = 25 fps)

AXIAL LOCATION, IN. (M)

1.0 (0.0254)   3.5(0.089)   5.0(0.127)   8.0(0.203)   12.0(0.305)   15.0(0.381)   17.5 (0.445)
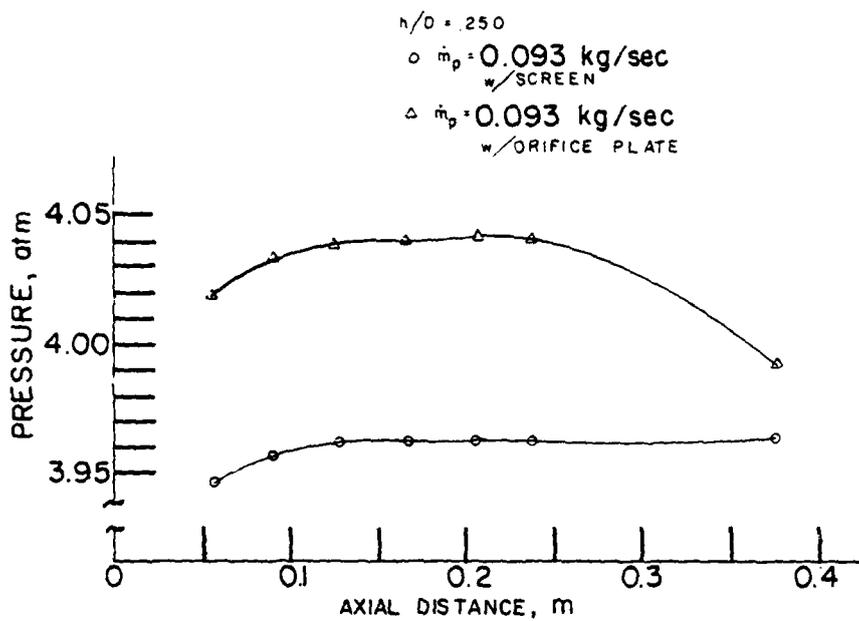
Fig. 16. Axial Pressure Distributions, Screen and Aft Orifice
Plate

42
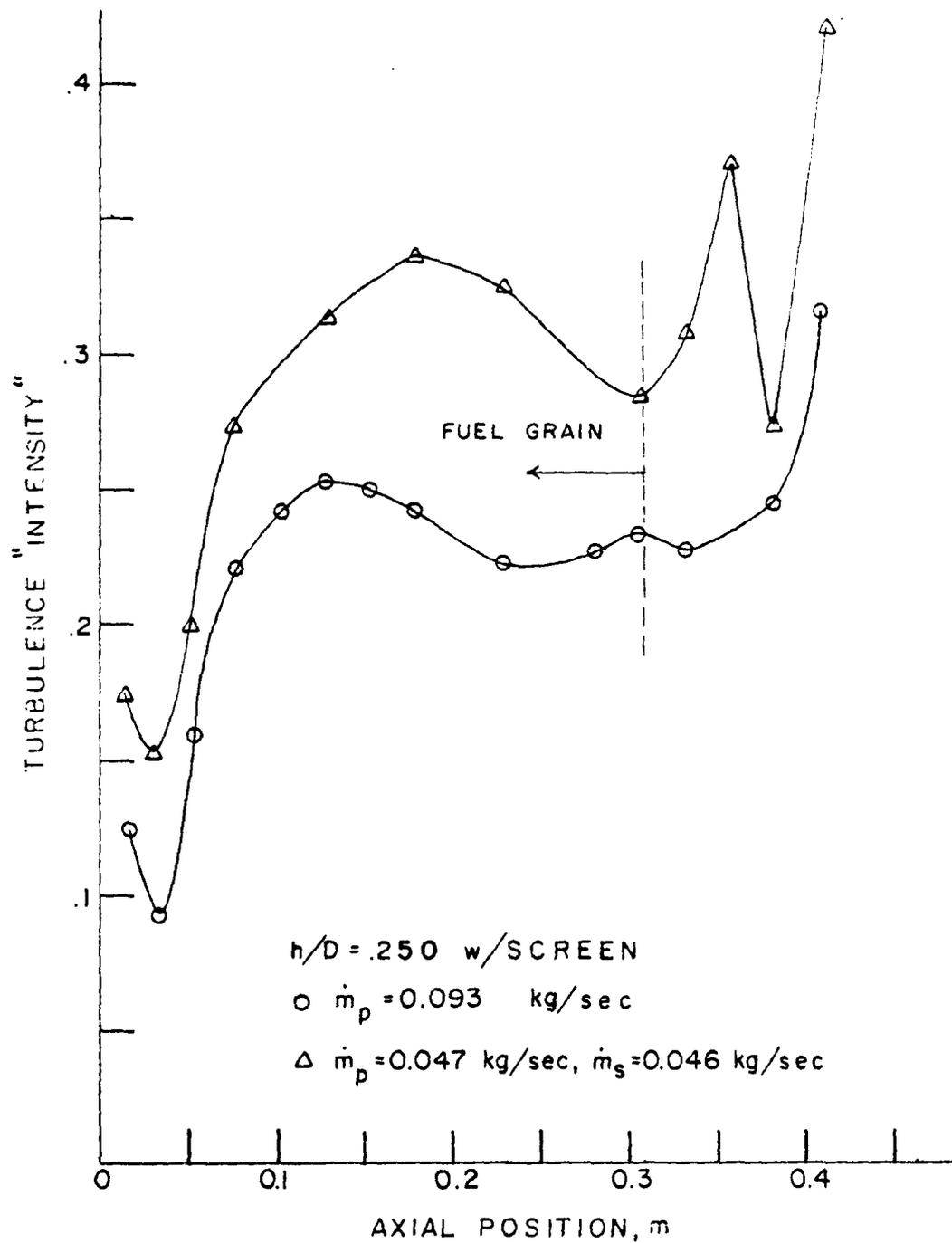
Fig. 17.   Centerline Turbulence Intensity, Inlet Screen
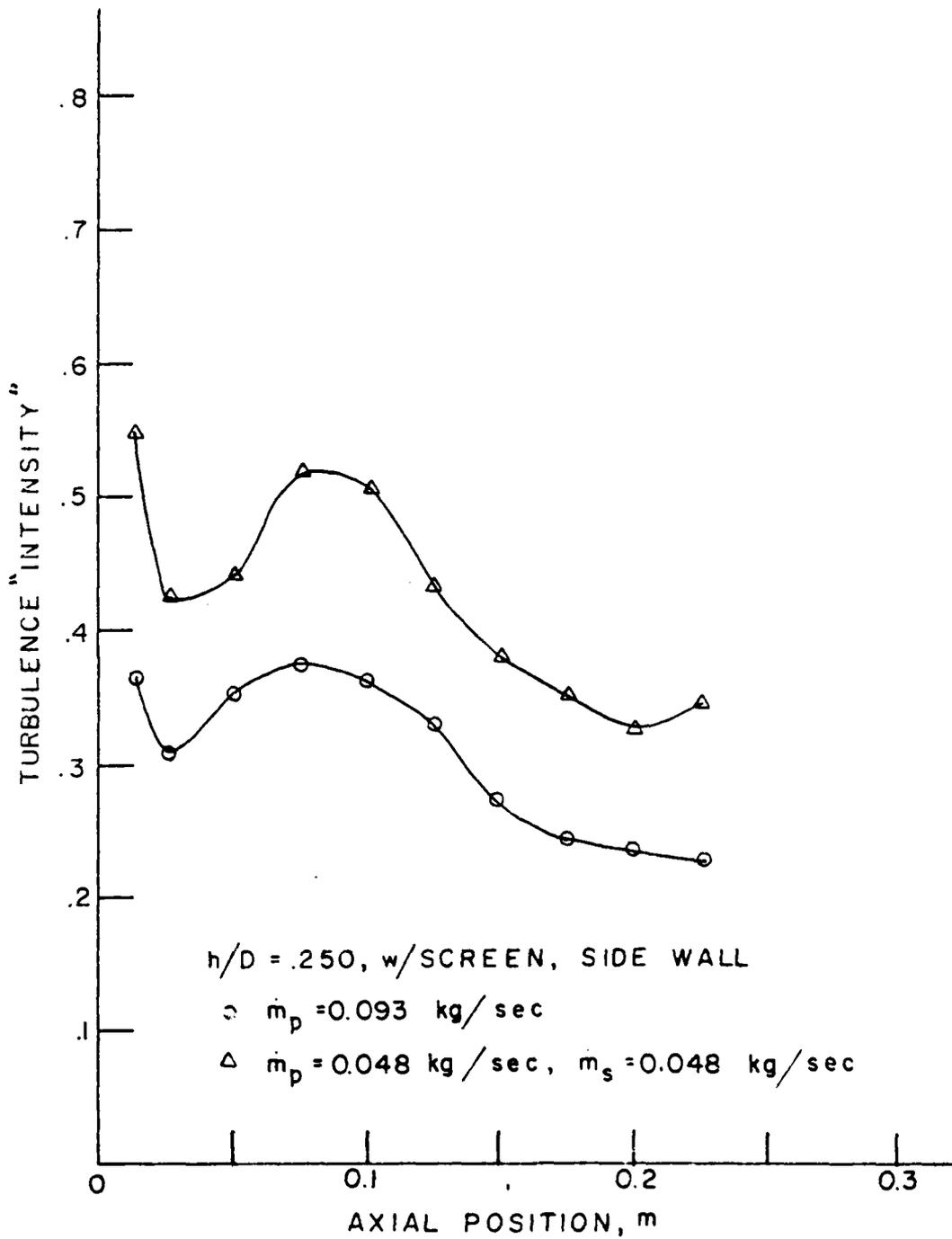
Fig. 18. Side Wall Turbulence Intensity, Inlet Screen

Fig. 19.   Bottom Wall Turbulence Intensity, Inlet Screen

45

AXIAL LOCATION, IN. (M)

1.0(0.0254)   3.5(0.089)   5.0 (0.127)   8.0(0.203)   10.5 (0.267)   13.0(0.330)   17.5 (0.445)
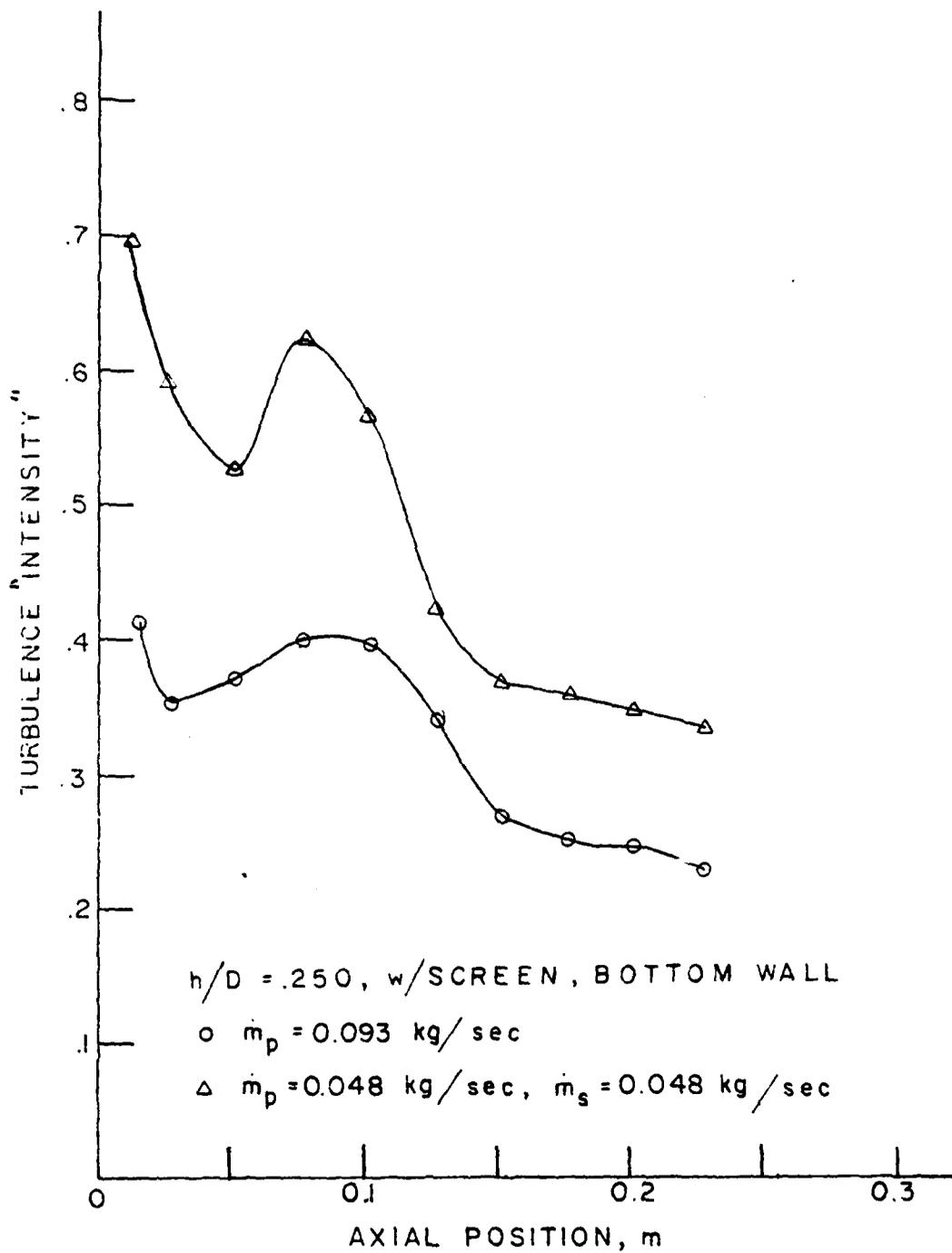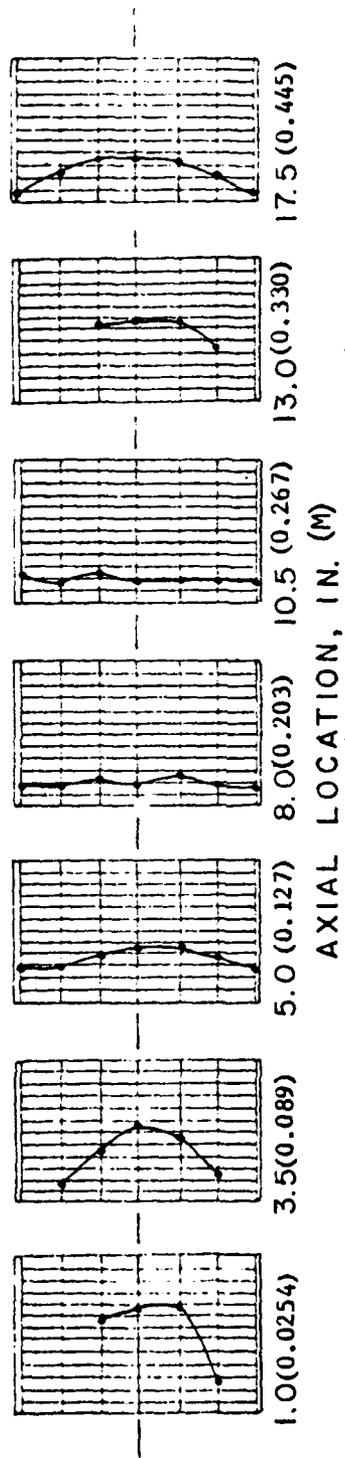
Figure 20.   Velocity Profiles, (Config. 8, Table I), w/Aft Orifice Plate, P_c = 4.04 atm,
$\dot{m}_p$ = 0.093 kg/sec (1 Div. = 25 fps)

46
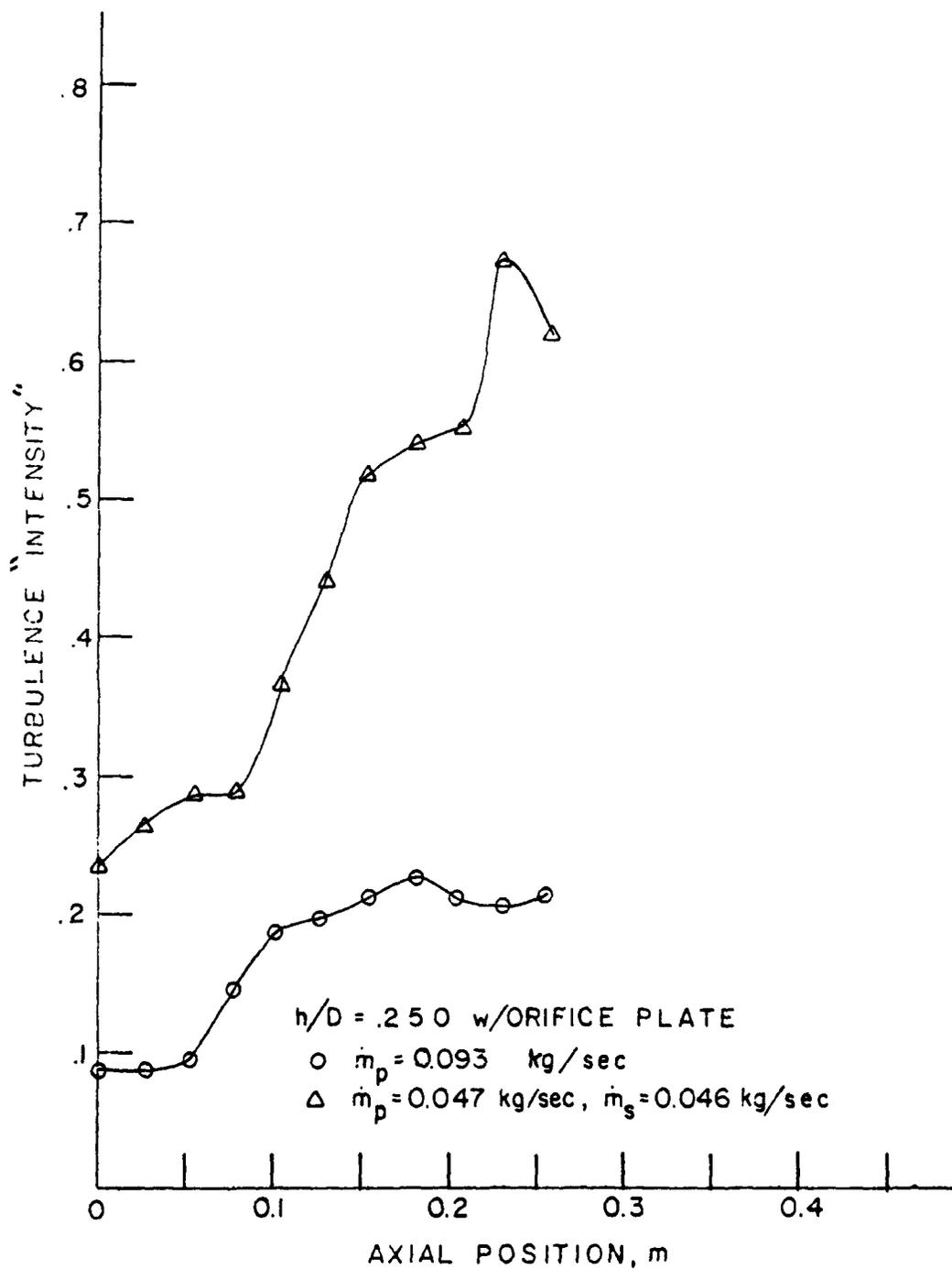
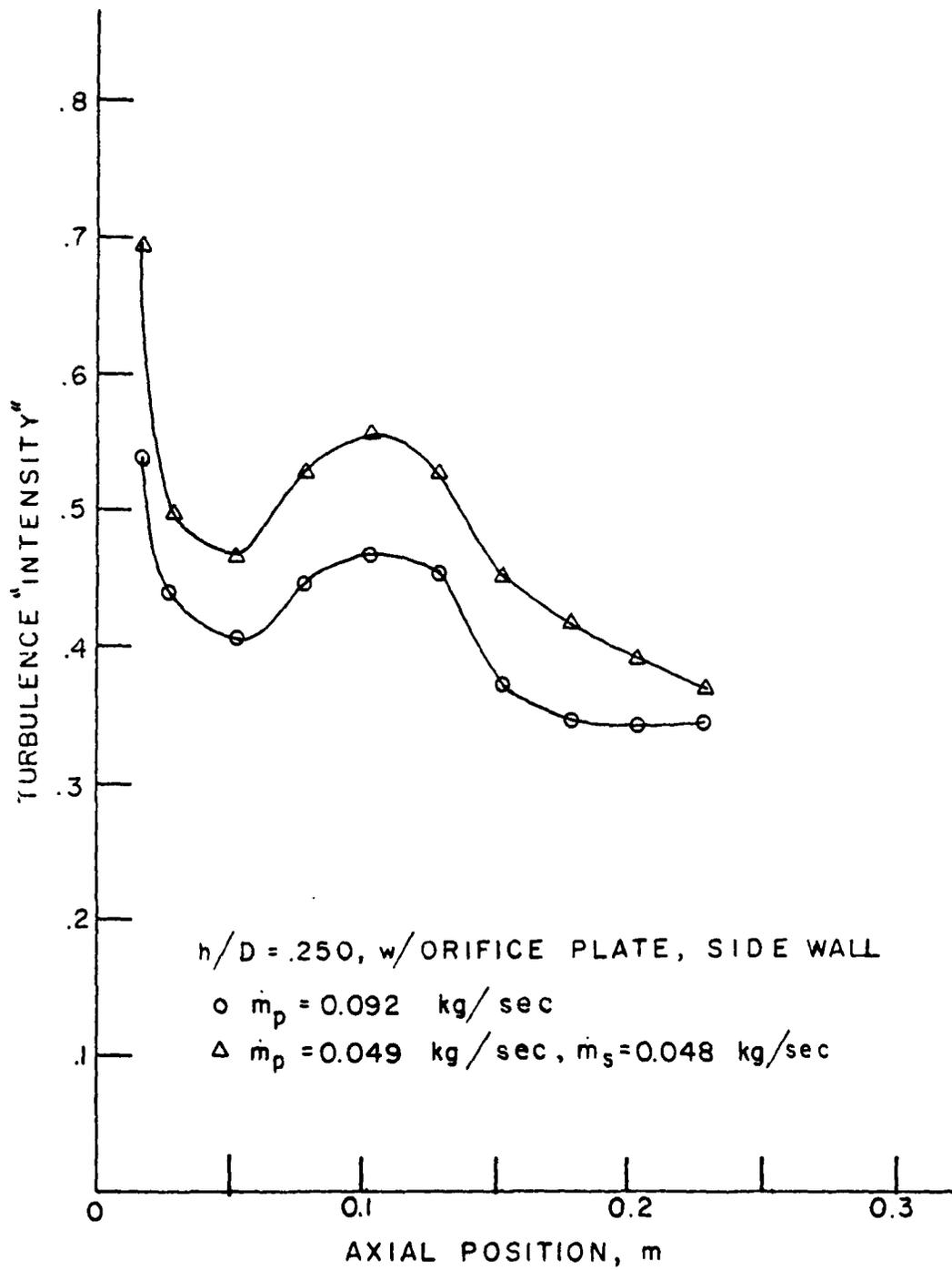Fig. 21. Centerline Turbulence Intensity, Aft Orifice Plate

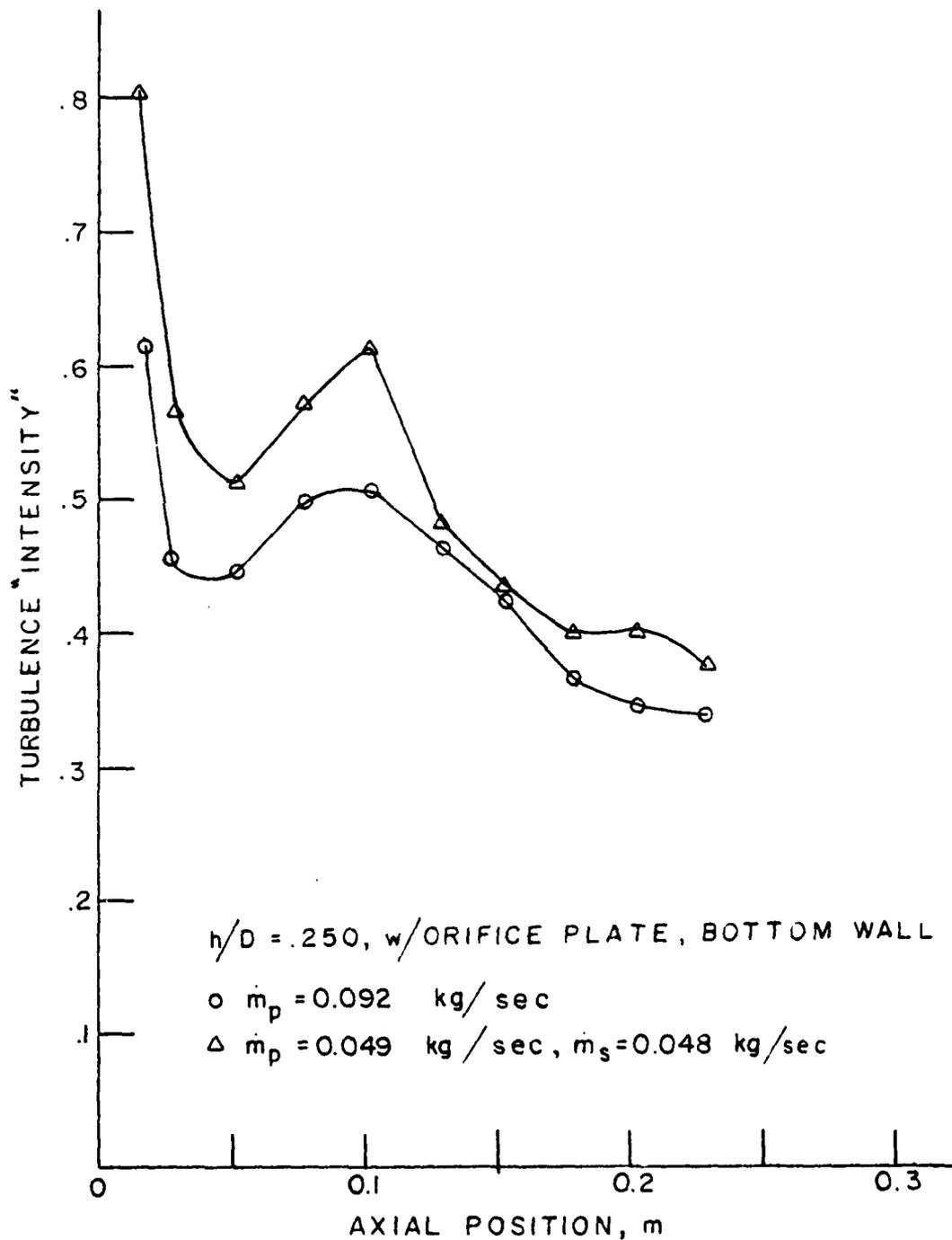Fig. 22. Side Wall Turbulence Intensity, Aft Orifice Plate

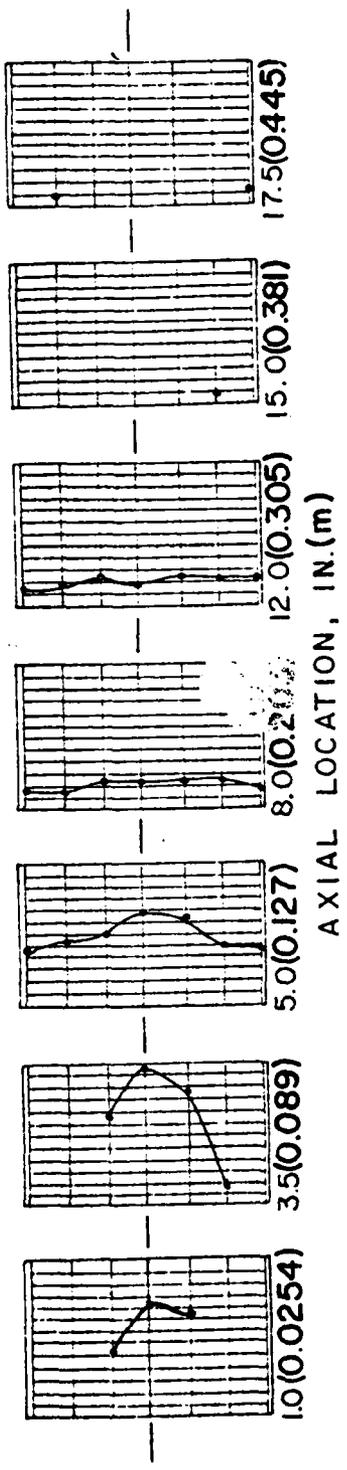Fig. 23. Bottom Wall Turbulence Intensity, Aft Orifice Plate

Fig. 24. Velocity Profiles, No-Bypass (Config. 3, Table 1), P_c = 4.06 atm, $\dot{m}_p$ = 0.094 kg/sec

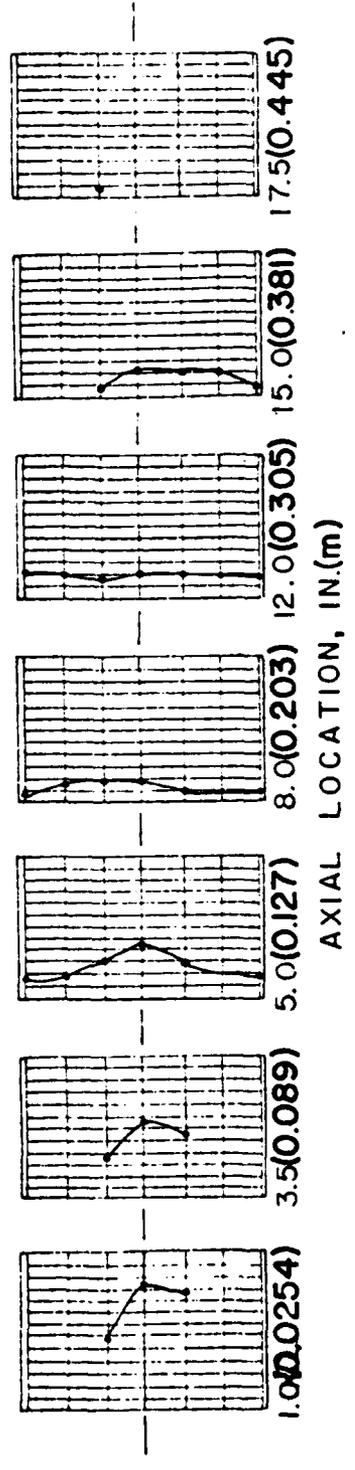(1 Div. = 25 fps ; at 1.0 in 1 Div. = 50 fps)

Fig. 25. Velocity Profiles, Bypass (Config. 4, Table 1), P_c = 4.10 atm, $\dot{m}_p$ = 0.049 kg/sec,
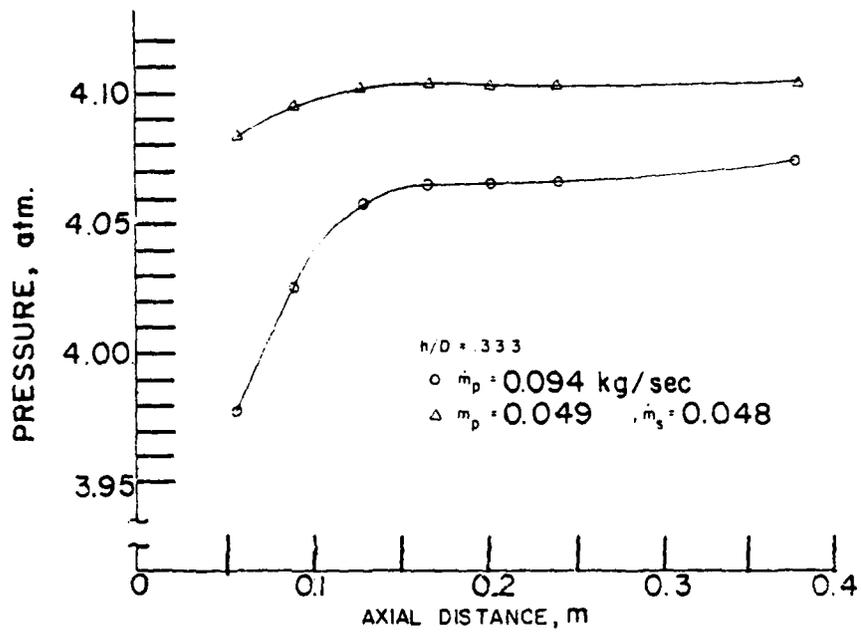
$\dot{m}_s$ = 0.048 kg/sec   (1 Div. = 25 fps)

50
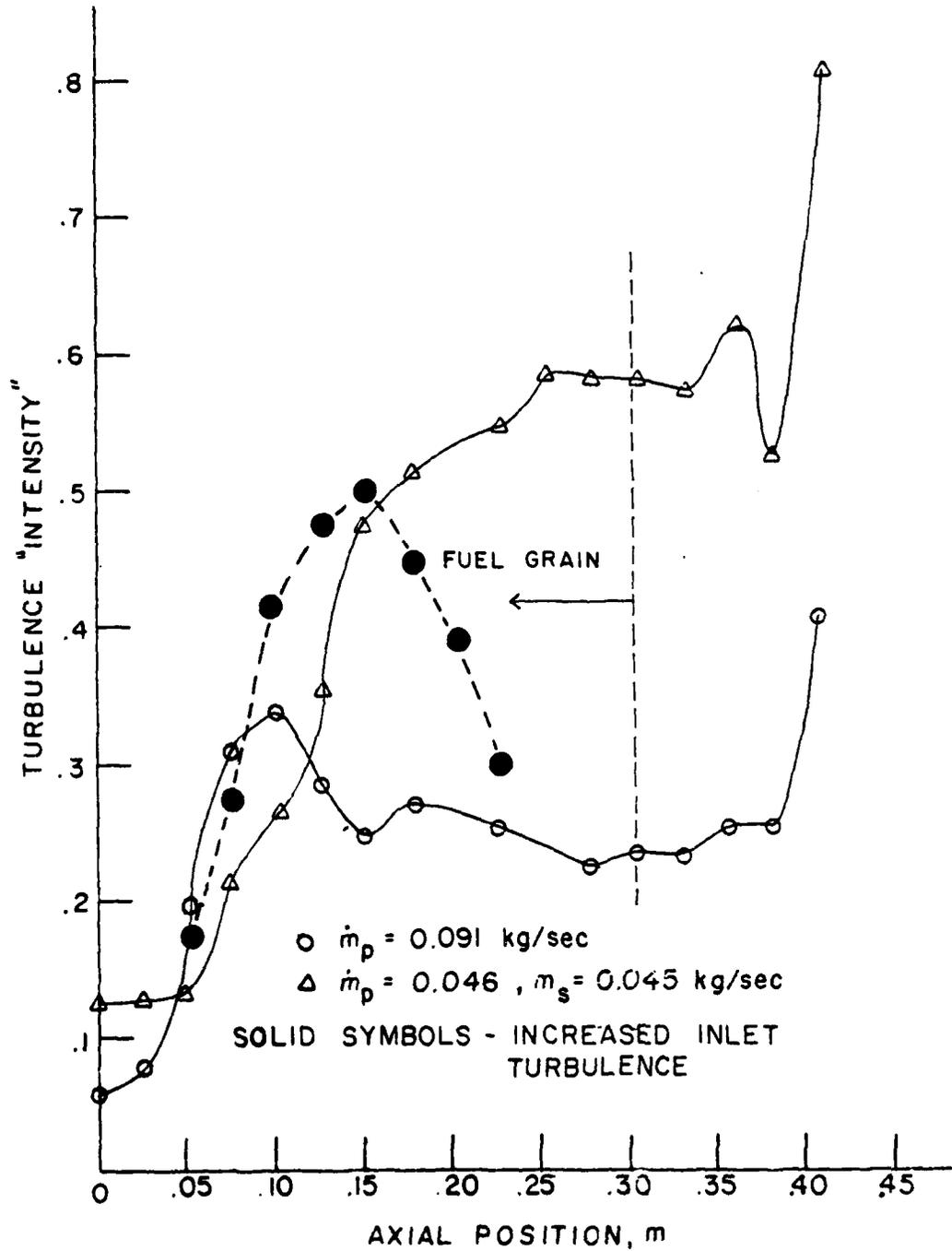
Fig. 26.   Axial Pressure Distributions, h/D = 0.333

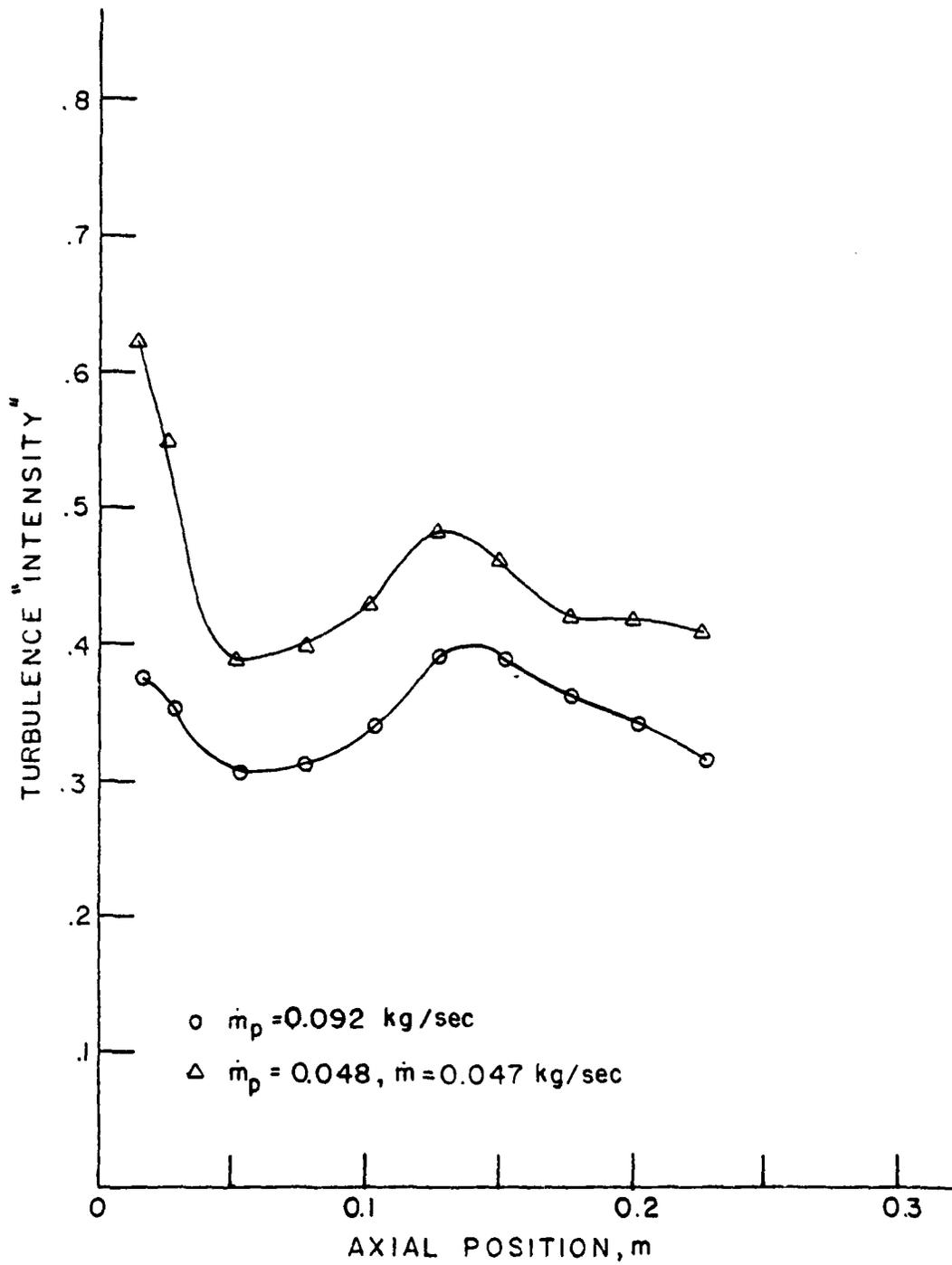Fig. 27. Centerline Turbulence "Intensity", h/D = 0.333

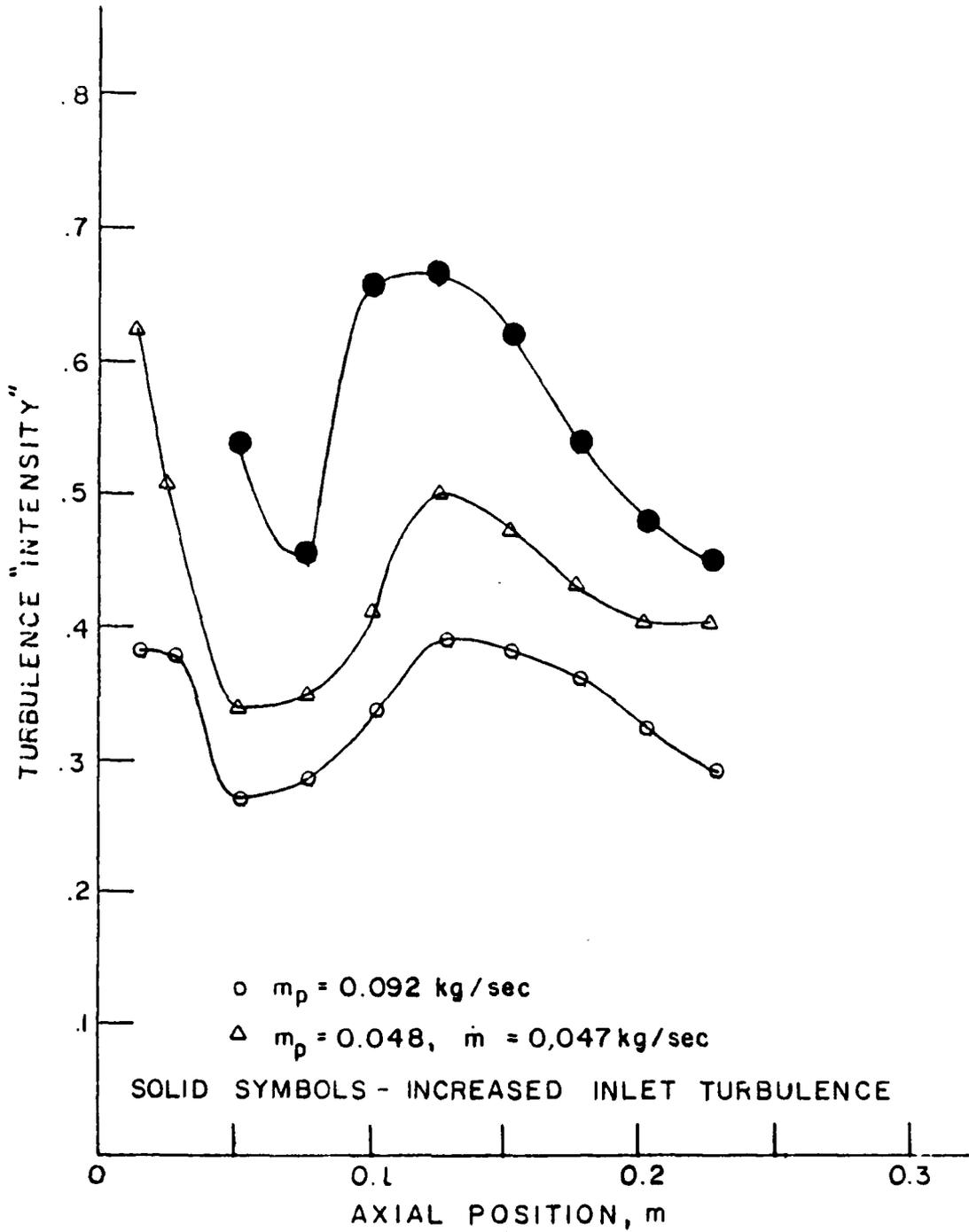Fig. 28. Side Wall Turbulence "Intensity", h/D = 0.333

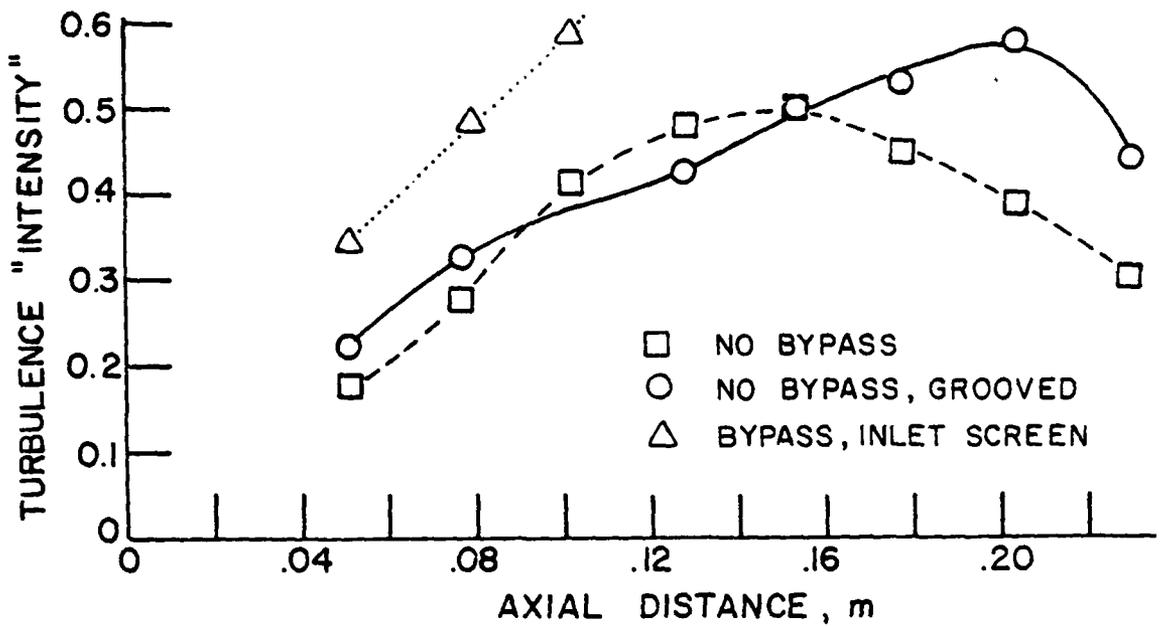53

Figure 29. Side wall Turbulence "Intensity", h/D = 0.333
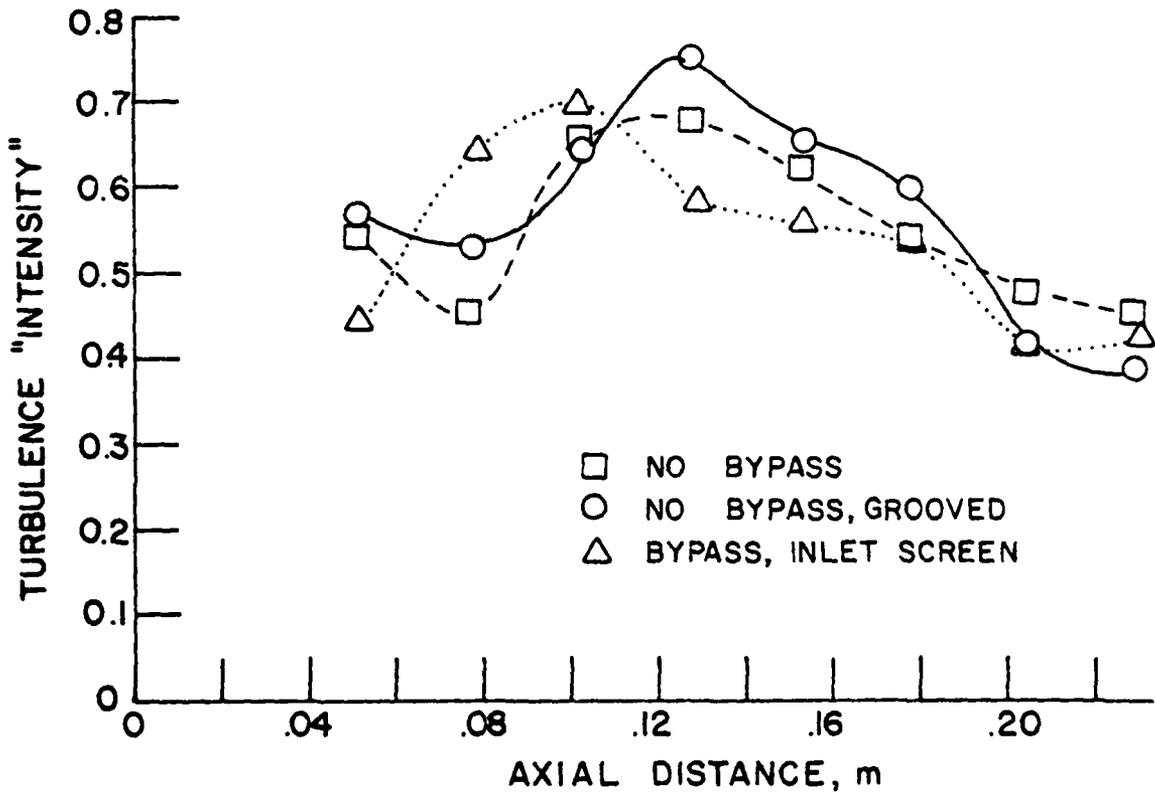
Fig. 30. Centerline Turbulence "Intensity" Profiles
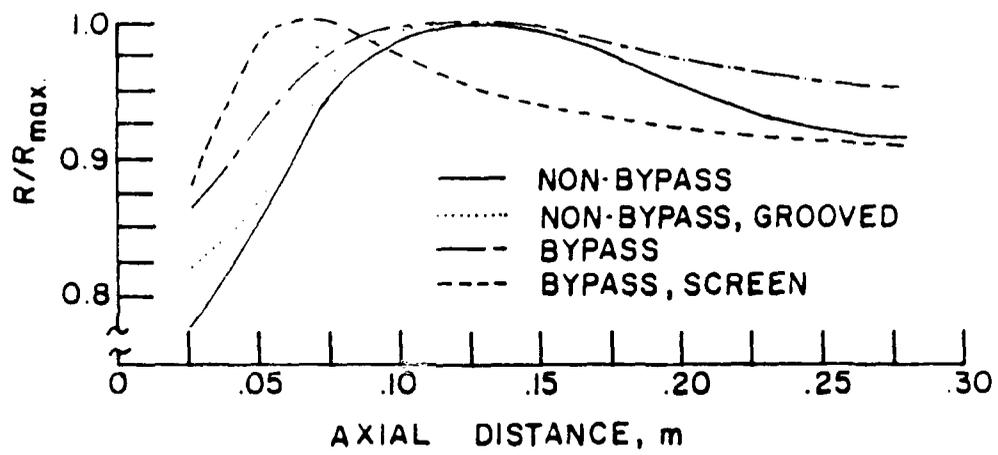

Fig. 31. Near-Wall Turbulence "Intensity" Profiles

55

Figure 32. Fuel Regression Rate Profiles

VII. REFERENCES

1. Netzer, D. W., "Modeling Solid-Fuel Ramjet Combustion," JSR, Vol. 14, No. 12, Dec. 1977, pp. 762-766.

2. Netzer, D. W., "Model Applications to Solid-Fuel Ramjet Combustion," JSR, Vol. 15, Sept-Oct. 1978, pp. 263-264.

3. Stevenson, C. A. and Netzer, D. W., "Primitive-Variable Model Applications to Solid Fuel Ramjet Combustion," JSR, Vol. 18, No. 1, Jan-Feb., 1981, pp. 89-94.

4. Boaz, L. D. and Netzer, D. W., "An Investigation of the Internal Ballistics of Solid Fuel Ramjets," NPS Report NPS-57Nt73031A, March 1973.

5. Phaneuf, Jr., J. T. and Netzer, D. W., "Flow Characteristics in Solid Fuel Ramjets," NPS Report NPS-57Nt74081, May 1974.

6. Mady, C. J., Hickey, P. J., and Netzer, D. W., "An Investigation of the Combustion Behavior of Solid Fuel Ramjets," NPS Report NPS-67Nt77092, Sep. 1977.

7. Mady, C. J., Hickey, P. J., and Netzer, D. W., "Combustion Behavior of Solid Fuel Ramjets," JSR, Vol. 15, No. 3, May-June 1978, pp. 131-132.

8. Hewett, M. E. and Netzer, D. W., "Application of Light Extinction Measurements to the Study of Combustion in Solid Fuel Ramjets," NPS Report NPS-67-78-008, Nov. 1978.

9. Hewett, M. E. and Netzer, D. W., "Light Transmission Measurements in Solid Fuel Ramjet Combustors," JSR, Vol. 18, No. 2, March-April 1981, pp. 127-132.

10. Burdette, W. and Reed, R., Jr., "Navy High Energy Solid Ramjet Fuel Program," 1979 JANNAF Propulsion Meeting, Anaheim, Ca, 5-9 March 1979.

11. Schadow, K. C., "Solid Fuel Ramjet Evaluation," 16th JANNAF Combustion Meeting, Monterey, CA, 10-14 Sep. 1979.

INITIAL DISTRIBUTION LIST

	No. of Copies
1. Library, Code 0212	2
Dean of Research, Code 012	2
Naval Postgraduate School	
Monterey, CA 93940	

2. Department of Aeronautics
   Code 67
   Naval Postgraduate School
   Monterey, CA   93940

Prof. M. F. Platzer, Chairman	1
Prof. D. W. Netzer	15
LT W. E. Scott	2
CAPT B. A. Binn	2

3. Defense Technical Information Center   2
   Attn: DDC-TCA
   Cameron Station, Bldg. 5
   Alexandria, VA   22314

4. Naval Air Systems Command   2
   Washington, D.C.   20361
      AIR-330

5. Naval Weapons Center
   China Lake, CA   93555

Tech. Library, Code 753	3
F. Zarlingo, Code 3246	3
K. Schadow, Code 388	1
W. Burdette, Code 3244	1

6. Chemical Systems Division
   United Technologies
   P.O. Box 358
   Sunnyvale, CA   94088

Tech. Library	1
R. Dunlap	1
A. Holzman	1
G. Jensen	1
P. Willoughby	1
P. LaForce	1

7. Chemical Propulsion Information Agency   2
   APL-JHU
   Johns Hopkins Road
   Laurel, MD   20810

8. AFAPL
   Wright-Patterson AFB, OH   45433
      R. D. Stull   2